ELSEVIER

International Journal of Mass Spectrometry 216 (2002) 1–27

International Journal of Mass Spectrometry

www.elsevier.com/locate/ijms

Review

Quantitative determination of noncovalent binding interactions using soft ionization mass spectrometry

Jürg M. Daniel, Sebastian D. Friess, Sudha Rajagopalan, Silke Wendt, Renato Zenobi*

Department of Chemistry, Swiss Federal Institute of Technology (ETH), ETH Hönggerberg HCI, CH-8093 Zurich, Switzerland

Received 27 December 2001; accepted 14 February 2002

Abstract

For a number of years, soft ionization mass spectrometry has been used for studying noncovalently bound complexes. An intriguing question in this context is whether MS experiments can be used to measure the interaction strength. A number of recent studies have addressed this question. The results of these studies, as well as the methods employed are reviewed here. We distinguish between liquid-phase methods such as mass spectrometrically detected melting curves, titration experiments, or competition experiments, and gas-phase methods such as cone voltage-driven dissociation, collision-induced dissociation, blackbody infrared radiative dissociation, or thermal dissociation of gas-phase complex ions. With a few exceptions, no agreement exists between solution-phase and gas-phase binding energies. The main reason is that electrostatic and dipolar noncovalent interactions are strengthened in the absence of solvent shielding, while other noncovalent interactions, in particular hydrophobic interactions, become less important in the absence of solvent. The possibility to quantitatively measure solution-phase as well as gas-phase noncovalent interaction strengths by mass spectrometry opens fascinating perspectives for very high sensitivity screening assays as well as for improved fundamental understanding of the nature of noncovalent interactions. (Int J Mass Spectrom 216 (2002) 1–27) © 2002 Elsevier Science B.V. All rights reserved.

Keywords: Noncovalent complex; Binding constants; MALDI; ESI; FAB; Soft ionization

1. Introduction

A number of established analytical methods are being used for the quantitative study of noncovalent macromolecular interactions. These all work in the solution phase and include optical spectroscopy (e.g., UV absorption, circular dichroism (CD), and fluorescence), nuclear magnetic resonance (NMR), light scattering, differential scanning calorimetry, and isothermal titration calorimetry [1]. Mass spectrometry is a novel tool for studying biomolecular structures and noncovalent interactions; it can provide data on the functional properties of biomacromolecules complementary to that obtained from more traditional techniques. Smith and coworkers have discussed the advantages and disadvantages of mass spectrometry compared to other biophysical methods for investigating noncovalent interactions [2,3]. For example, mass spectrometry has undisputed advantages over NMR for studying proteins with poor solubility and high molecular weight. NMR is limited to studies of proteins with a molecular weight less than 30,000 Da,

* Corresponding author. E-mail: zenobi@org.chem.ethz.ch

1387-3806/02/$ – see front matter
PII S1387-3806(02)00585-7

while mass spectrometry has been used to study proteins and protein complexes with molecular masses approaching 1,000,000 Da [4–7]. Unlike NMR or CD, techniques that measure average of properties of biomacromolecules, soft ionization mass spectrometry in connection with H–D exchange can provide detailed and quantitative information about the kinetics of protein folding [8].

McLafferty has often referred to the three "S" advantages of mass spectrometry: specificity, sensitivity, and speed [9]. Most importantly, the sensitivity of MS-based methods (picomole to femtomole range) allows the investigation of very small quantities of material, which renders MS a very useful method in cases where only a microgram or less of a valuable protein may be available for study. In addition, accuracy (±0.01%) and mass range of modern soft ionization MS methods are very useful. A fourth "S" advantage in the context of noncovalent interactions should include stoichiometry [10]: the number of ligands that form a unique and biologically relevant complex is an important issue in many such systems, a quantity that is easily obtained from mass spectrometry. Another great advantage of mass spectrometry as an analytical tool, especially applicable to the identification of unknown molecules, is the possibility to carry out tandem mass spectrometry experiments or even MS, leading to an exponential increase in data and information [11].

2. MS techniques for detecting noncovalent complexes

Soft ionization mass spectrometry, in particular matrix-assisted laser desorption/ionization (MALDI) and electrospray ionization (ESI), has led to a revolution in the application of MS methods to high molecular weight biomolecules, to synthetic polymers, and to many other classes of compounds that were previously not accessible to mass spectrometric investigation. Protein and peptide detection and sequencing, DNA sequencing, protein folding, assessing the contribution of individual amino acid residues to a protein's function, in vitro drug analysis, and drug discovery are among the areas to which MALDI and ESI have been applied with great success (for a review, see [12]). In MALDI, the sample is cocrystallized at fairly high dilution with a chemical matrix. Upon exposure to pulsed laser radiation, the matrix sublimates and carries the analyte molecules into the gas phase [13–15]. During this process, ions are formed or liberated in a variety of mechanisms [16]. In ESI (Fig. 1), the sample is sprayed directly from solution by a strong electric field gradient [17,18]. An ESI mass spectrum typically shows a distribution of multiply charged ions. An intrinsic property of all mass analyzers is that they separate ions according to their mass-to-charge (m/z) ratio, not mass.

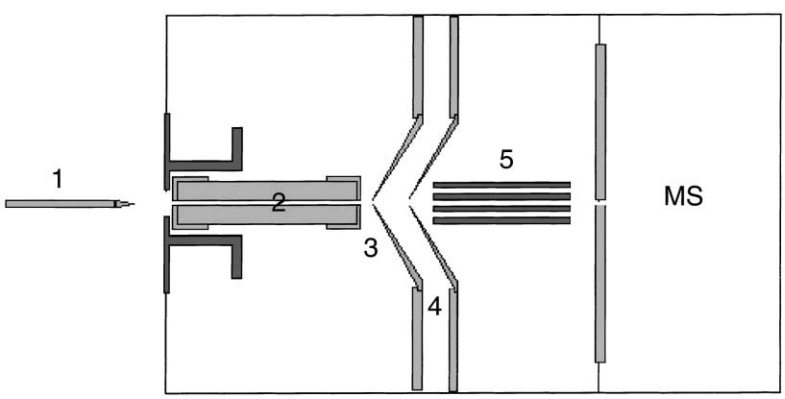

Fig. 1. A typical electrospray ion source; (1) the spray capillary, (2) a heated transfer capillary leading to the first stage of differential pumping. In some configurations, the transfer capillary 2 consists of two segments for thermal dissociation of gas-phase complexes, (3) and (4) the differential pumping stages, (5) an octopole ion guide inside pumping stage 3. Thereafter, the ions are guided to the mass analyzer.

Hence, an advantage of multiple charging is that a mass analyzer with a relatively small m/z range (e.g., quadrupole instruments) can be used to observe very large molecules.

Much less known but perhaps even more interesting is the fact that soft ionization methods allow, under certain conditions, the transfer of noncovalently bound complexes into the gas phase, and therefore the mass spectrometric determination of their stoichiometry and sometimes mode and energy of interaction. Ganem et al. [19] were the first to describe the use of a soft ionization method, ion spray mass spectrometry, for the identification of noncovalent host–guest interactions, more precisely, the noncovalent binding of macrolide immunosuppressors to a cytoplasmic receptor. Ion spray has since been replaced by ESI, which is the predominant method used for mass spectrometric investigation of noncovalent complexes; MALDI mass spectrometry is applied much less frequently.

A third method introduced recently, called laser-induced liquid beam ionization/desorption (LILBID) [20], has also shown promise for the detection of high mass biomolecules, their clusters, as well as specific noncovalent complexes [21–23]. In this method, a laser beam desorbs species directly from a liquid jet of solution sprayed into a specially designed ion source. LILBID requires custom designed instruments and is, until now, in use only in the laboratory of its inventors. Before ESI and MALDI became established techniques, fast atom bombardment (FAB) was occasionally used for the determination of solution-phase stability constants of noncovalent complexes [24–26]. These early FAB studies were limited to crown ether–alkali metal systems and to solvents that represent typical FAB matrices, mostly glycerol, or sometimes glycerol/water mixtures. Other limitations of FAB include the relatively low upper mass limit of a few 1000 Da only, and a notable degree of fragmentation. Electrohydrodynamic mass spectrometry (EHMS), another precursor to ESI, has also been used to study complexation equilibria quantitatively. Man et al. [27] measured the relative stability constants of 18-crown-6 with various metal cations in glycerol by EHMS.

Review articles by Smith and Zhang [2], Przybylski and Glocker [28], Winston and Fitzgerald [8], Smith et al. [29], Loo [10], Pramanik et al. [30] on ESI–MS and by Hillenkamp [31] on MALDI–MS as applied to noncovalent complexes have been published. It is normally a greater challenge to apply MALDI–MS to noncovalent complexes, because the weak interaction forces have to survive both the sample crystallization as well as the laser desorption/ionization event. MALDI is therefore believed to be somewhat less “soft” than ESI.

Noncovalent interactions can come in many different flavors. Table 1 gives a summary of the types of noncovalent interactions that occur between particles that are either charged, carry a dipole moment, or are polarizable [32].

The equations given in Table 1 give the free energies of interaction. Coulomb interactions between two charges are long-range and strong, and can be attractive or repulsive, dependent on the sign of the charges involved. Dipole–dipole interactions can also be attractive or repulsive, dependent on the relative angular orientation of the interacting dipoles. All other interactions are attractive because permanent or induced dipoles can orient to accommodate the forces acting on them. Even particles without any charge or dipole moment can attract themselves, by virtue of their polarizability (London dispersion force). A rough classification can be made according to the distance dependence of noncovalent interactions, which varies between a $1/r$ distance dependence for the Coulomb energy to the well known $1/r^6$ distance dependence for all van der Waals free energies. Another important fact to note is that all interaction energies contain a $1/\varepsilon$ term, i.e., in the presence of a medium with high dielectric constant such as water, the interaction energy drops by an appropriate factor. This is an important consideration when comparing solution-phase with gas-phase interaction energies, where the solvent medium is absent. Interaction energies based on charges, dipoles, and polarizability are thus expected to increase when going from solution into the gas phase. A notable exception is the hydrophobic interaction, which is an unusually strong attraction

Table 1
Types of noncovalent interactions

Type of noncovalent interaction	Formula	Name
Charge–charge	$\frac{Q_1 Q_2}{4\pi\varepsilon\varepsilon_0 r}$	Coulomb energy
Charge–dipole (fixed dipole)	$-\frac{Qu\cos\theta}{4\pi\varepsilon\varepsilon_0 r^2}$	
Charge–dipole (freely rotating dipole)	$-\frac{Q^2u^2}{6(4\pi\varepsilon\varepsilon_0)^2kTr^4}$	
Dipole–dipole (fixed dipole)	$-\frac{u_1u_2}{4\pi\varepsilon\varepsilon_0 r^3}(2\cos\theta_1\cos\theta_2 - \sin\theta_1\cos\phi\sin\theta_2)$	
Dipole–dipole (freely rotating dipole)	$-\frac{u_1^2u_2^2}{3(4\pi\varepsilon\varepsilon_0)^2kTr^6}$	Keesom energy (van der Waals energy $\propto 1/r^6$)
Charge–nonpolar	$-\frac{Q^2\alpha}{2(4\pi\varepsilon\varepsilon_0)^2r^4}$	
Dipole–nonpolar (fixed dipole)	$-\frac{u^2\alpha(1+3\cos^2\theta)}{2(4\pi\varepsilon\varepsilon_0)^2r^6}$	
Dipole–nonpolar (freely rotating dipole)	$-\frac{u^2\alpha}{(4\pi\varepsilon\varepsilon_0)^2r^6}$	Debye energy (van der Waals energy $\propto 1/r^6$)
Nonpolar–nonpolar	$-\frac{3}{2}\frac{\alpha_{01}\alpha_{02}}{(4\pi\varepsilon\varepsilon_0)^2r^6}\frac{I_1I_2}{I_1+I_2}$	London dispersion energy (van der Waals energy $\propto 1/r^6$)
Hydrogen bond	Special, directed interaction	
Hydrophilic interaction	Special interaction	
Hydrophobic interaction	Special interaction	

Adapted from Israelachvili [32]. Q = charge, u = dipole, r = distance, α = polarizability, ε = dielectric constant, I = first ionization potential, θ = angle between dipole and vector connecting the interacting particles, ϕ = polar angle of second dipole.

between two hydrophobic binding partners in water. Conversely, in the absence of solvent, a hydrophobic interaction is substantially weaker. Like hydrophobic interactions, hydrophilic interactions and hydrogen bond interactions are not readily described by a simple formula. Hydrogen bonds are directed interactions of primarily electrostatic nature, worth about 10–40 kJ mol^{-1}. Both hydrophobic interactions and hydrogen bonds are of great importance for the three-dimensional structure of biomacromolecules, as well as for the formation of noncovalent complexes.

2.1. Is it possible to determine noncovalent interaction energies by mass spectrometry?

As we have already seen, the detection of noncovalently bound assemblies by mass spectrometry is fairly well established. A recurring question concerns the applicability of MS methods to measuring noncovalent interaction strengths. This review aims to answer this question, by clarifying what exactly is being determined by various MS-based methods, and by presenting a number of examples. We are concentrating on noncovalent interactions involving biomolecules and biopolymers – peptides, proteins, enzymes, oligonucleotides, oligosaccharides, etc., and their interactions with other large or small molecular species, e.g., enzyme inhibitors. We have thus virtually excluded the topic of metal ion binding to small organic ligands. For the most part, such complexes pose no particular problems to study by mass spectrometry. Modern soft ionization methods are not required; rather, the challenge lies in determining metal ion–ligand binding interactions more and more precisely. Metal ion–ligand complexes have been studied extensively using mass spectrometry methods, and excellent reviews are available (e.g., see [33]).

2.2. Specificity of noncovalent interactions

A peak at the mass of an alleged complex is not a sufficient criterion to prove its specificity, it might in fact be a false positive [34]. Key to determining the specificity of noncovalent interactions are suitable controls. Controllable factors need to directly influence the outcome of the MS data, otherwise the mass spectrum does not reflect the investigated system properly [35]. There are number of ways to test the specificity of noncovalent complexes [29], the two most important being chemical and experimental strategies.

Chemical strategies most often involve judicious modification in the sequence of biopolymers that weaken or disable noncovalent interactions, e.g., base mismatch in oligonucleotides, covalent modification of amino acid residues in peptides, or the use of mutant proteins. The corresponding signals in the mass spectrum must decrease or disappear completely. Selective covalent modification reactions exist for a variety of amino acids: lysine residues can be converted to homo-arginine [36], cysteine thiols can be trimethylamino-ethylated to thialamine [37], comparable routines exist for histidine [38] and more general methods such as methylation or acetylation have been applied as well [39]. Disulfide bonds generally survive enzymatic digests, thus disulfide-bonded fragments and their reduced-free forms allow verification of the cysteine locations [40]. Recently, an elegant way for masking the amino terminus has been presented [41]. A simple alternative to covalent modification is the use of commercial mutants to scan various sequences for their specific interactions [42]. Amide protons next to reactive amino acid residues may sometimes participate in complex formation that involves the protein backbone, thus the use of proline at such a position is a useful strategy to disrupt backbone interactions [43]. An interesting example has been presented by Rostom et al. [44]: they characterized peptide binding properties of a periplasmic peptide receptor by using different amino acids, stereochemical features, different side-chain properties, and acetylation of the amino terminus of the peptides. Binding to the receptor was found to be insensitive to these chemical modifications, showing that the suspected binding site could not be confirmed. The authors concluded that the bound peptides were encapsulated by the receptor in a solvent-filled cavity and supported this interpretation with further evidence from mass spectral peak widths and from the charge state distribution in the ESI mass spectra.

Experimental strategies include different sample preparation techniques [45] or denaturation as a tool to induce conformational changes [46]. Comparative experimental strategies such as change in temperature or different buffer systems have been described early on by Smith and Light-Wahl [47]. Using this strategy, the specificity of zinc finger peptide–oligodeoxynucleotide complexes was demonstrated [48], whereas only unspecified binding between cyclodextrins and a variety of compounds that could potentially form inclusion complexes was found in a MALDI mass spectrometry study [49]. Recently, the comparison of MALDI and ESI data of identical systems has been found to be attractive in this respect, too [50–53]. Clearly, if the mass spectral data should reflect solution conditions, the degree of complexation must not depend on the ionization method used.

When reasoning about the specificity of a complex binding interaction in a mass spectrometry experiment, an implicit assumption is that folded biomolecules participating in this interaction retain a near-native conformation in the gas phase. This is, however, difficult to prove directly. Usually, it is based on fairly indirect evidence, although structurally sensitive MS methods are beginning to emerge [42,43,46,54–57]. An interesting, somewhat more direct way to demonstrate the existence of near native structural elements in gas-phase biomolecules was described by Fenselau and coworkers [58,59]. They measured the kinetic energy release upon dissociation of multiply charged polypeptide ions in a mass-analyzed ion kinetic energy (MIKE) experiment. The relatively large kinetic energy release was thought to be due to Coulombic repulsion between the charges on the fragments. These authors compared experimental values with calculated Coulombic repulsion obtained from molecular dynamics models, and found very

good agreement. This led them to conclude that the α-helical secondary structure of mellitin [58] as well as multistrand β-pleated sheets [59] survive in the gas phase, whereas single β-strands, e.g., in a polyalaline 16-mer or in bombesin, form collapsed structures.

3. Possibilities to determine noncovalent interaction strengths by MS

In this chapter, methods based on mass spectrometry for determining noncovalent binding strengths are reviewed. We distinguish between solution-phase methods with MS detection and gas-phase methods where the complex is dissociated in the mass spectrometer. In this article, we distinguish between the terms "fragmentation" and "dissociation:" with the latter, we describe the rupture of the noncovalent interaction, while the former implies breaking of covalent bonds of the binding partners.

3.1. Solution-phase methods with MS detection

Conceptually, the simplest way of determining stability constants with a mass spectrometer is to use it as a detector for solution-phase chemistry. It is necessary to ensure that solution-phase parameters, and not gas-phase properties, are actually measured in such an experiment. For instance, it must be avoided that a noncovalent complex partially dissociates in the mass spectrometer after being transferred to the gas phase. ESI–MS has been shown to meet these requirements; appropriately treated, ESI–MS can be used to determine solution-phase parameters [10,60–66]. Another very important condition is that the ion formation process does not disturb the solution-phase equilibria. In ESI–MS, for example, it can be imagined that the changes in pH and ion strength in a shrinking microdroplet shift the position of the equilibrium dramatically. In an insightful study by Wang and Agnes [67], this question was addressed using the complexation of strontium with EDTA ($Sr^{2+} + EDTA^{4-} \leftrightarrows Sr\text{–}EDTA^{2-}$), where the forward reaction rate is much faster ($10^9\,M^{-1}\,s^{-1}$) and the reverse reaction rate is much slower ($1\,s^{-1}$) relative to the time scale of the ESI process ($\approx 10^{-2}$ s). A shift of the equilibrium to the right, representing the dynamic changes of the equilibrium due to passage through the ion source was expected. However, these authors found that the deviation in the position of the equilibrium compared to solution phase was smaller than expected, and that monitoring of kinetically labile species by ESI is straightforward. This is a very important issue and we feel that there is an urgent need that it is studied more extensively.

3.1.1. Melting curves

A common method to determine noncovalent interaction strength, most often used in the field of oligonucleotide chemistry, is measuring the melting curve of a complex in solution. The fraction of intact complex, α, is determined as a function of solution temperature. Detection is normally done optically, using UV absorption, fluorescence, or circular dichroism. From the slope of the melting curve, a transition enthalpy can be derived according to [68],

$$\Delta H = (2 + 2n)RT_{\mathrm{m}}^2 \left(\frac{\partial \alpha}{\partial T}\right)_{T=T_{\mathrm{m}}} \quad (1)$$

where n is the molecularity of the association reaction (e.g., $n = 2$ for dimerization) and T_{m} is the melting temperature, normally defined for $\alpha = 50\%$. A mass spectrometric analog of this approach has been described in the literature. In its simplest implementation, the sample solution is at a defined temperature that is slowly raised during the course of the experiment, and α is measured mass spectrometrically. The same can be achieved by controlling the temperature of the spray capillary in an ESI source (see Fig. 1), an option that some manufacturers provide for their instruments. This should not be confused with the "heated capillary method" where the transfer capillary is at elevated temperature. The latter is a gas-phase dissociation method that will be discussed, while the former is only affecting the temperature of the spray solution, thus measuring solution-phase stability.

An early example of measuring oligonucleotide solution stability constants by MS has been presented

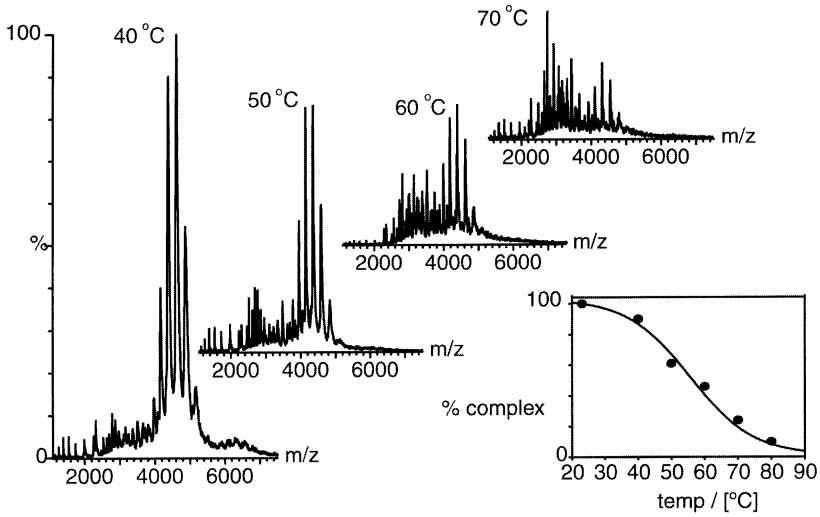

Fig. 2. Thermal dissociation of MtGimC monitored by mass spectrometry. Each sample was equilibrated at the desired temperature for 15 min before recording the ESI mass spectrum. Peaks corresponding to intact MtGimC appear between $m/z = 4000$ and 5000, while dissociation products mostly show up at lower m/z. The fraction of complex was calculated from the sum of the intensity of the ions assigned to the complex signal relative to the total ion counts in each of the spectra (inset). Reproduced with permission from [70]. Copyright 2000, National Academy of Science, USA.

by Smith and coworkers [69]. They constructed complementary 2′,5′-linked DNA strands and compared their dissociation in solution with the stability of the natural DNA duplexes of identical base composition. Observing heterodimer formation through Watson–Crick base-pairing, the authors determined the relative stabilities of the 2′,5′- and the 3′,5′-linked duplexes by ESI–MS and found a qualitative agreement with complementary solution-phase stability measurements. They finally translated their data into a melting curve, i.e., a plot of the spray capillary temperature vs. the mole fraction of single and double strands.

Another remarkable example, the study of the effect of elevated temperature on the structure of the chaperone GimC/prefolding homologue complex, has been presented by Fändrich et al. [70]. The authors built a nanoflow device that allowed a reliable adjustment of the temperature of the solution containing the hexameric analyte. When increasing the temperature from 60 to 70 °C, the relative intensity of the signal assigned to the intact hexamer decreased, while that of the dissociation products increased. Peaks corresponding to the intact hexamer appeared between 4 and 5 kDa, while those of dissociation products were found below this m/z range (see Fig. 2).

The inset in Fig. 2 presents the results from the ESI–MS spectra in the form of a melting curve: the fraction of complex present was calculated from the sum of the intensity of the ions assigned to the complex and expressed as the percentage of the ion intensity of the hexamer (100%) under ideal physiological conditions. A solution melting (denaturation) temperature of around 60 °C was found for 50% intact complex, in good agreement with data from CD and gel-filtration experiments.

3.1.2. Titration

A typical use of ESI–MS is to monitor a solution-phase titration for the determination of the equilibrium of a host–guest pair. Generally, the host concentration is kept constant whereas the guest concentration is varied over a range of about two orders of magnitude. The intensity of the complex is then compared to the intensity of the free host for every ligand concentration. This will only work under the assumption that the ionization process does not affect

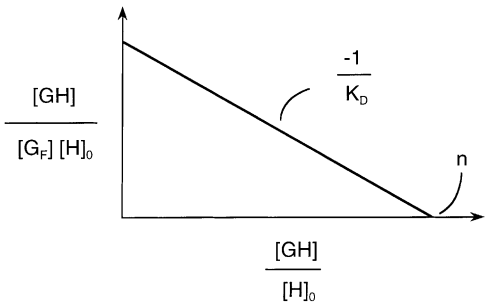

Fig. 3. Schematic of a Scatchard plot.

the equilibrium. Often graphic linearization such as Scatchard plots are used for the determination of association or dissociation constants. The ratio of bound (GH) over free guest (G_F) is plotted against the concentration of bound guest, which gives a linear relationship with slope $-1/K_D$ (see Eq. (2) and Fig. 3). If the total host concentration, $[H]_0$, is known, the data can be plotted as

$$\frac{[GH]}{[G_F][H]_0} = \frac{-1}{K_D}\frac{[GH]}{[H]_0} + \frac{n}{K_D} \quad (2)$$

where n represents the stoichiometry, i.e., the number of guests bound to one host molecule. If there is more than one binding site, an analysis by a Scatchard plot assumes that these are equivalent and independent.

One of the first examples using this method was presented by Lim et al. [71]. They used negative mode ion spray mass spectrometry to study binding of the glycopeptides vancomycin and ristocetin to a peptide (Ac_2KAA), representing the carboxyl terminus of a bacterial cell-wall protein. The concentration of the antibiotic was kept constant and titration was done by adding Ac_2KAA. From a calibration curve where the Ac_2KAA ion signal intensity is plotted vs. [Ac_2KAA] (found to be linear over a range of 0.25–20 μM) the concentration of the unbound Ac_2KAA could be determined. From these data a Scatchard plot was constructed, which gave binding constants (e.g., 6.25×10^5 for ristocetin–Ac_2KAA by MS) in good agreement with binding constants from solution-phase methods (5.9×10^5 for the same system). The correct stoichiometry of the complexes was also obtained. These authors observed a linear increase in complex signal with increasing concentration of the peptide Ac_2KAA up to equimolar stoichiometry. A problem of this early work was that 50% acetonitrile was added prior to analysis, representing conditions far from physiological ones. The agreement between the solution-phase binding constant and the value determined by mass spectrometry should thus be regarded with caution, and it should perhaps be clarified whether this is not simply a coincidence.

In solution-phase methods, it is sometimes difficult to recognize binding to two or more different sites, whereas the stoichiometry is easily obtained in MS experiments, because it is the molecular weight that is measured. Using ion spray MS to study the interaction of bovine serum albumin (BSA) with oligonucleotides, Greig et al. [72] identified two different, independent binding sites and determined the dissociation constants using a fit to a second-order polynomial [73]:

$$\frac{[H] + [HG] + [HG_2]}{[H]} = \frac{[G]^2}{K_{D1}K_{D2}} + \frac{[G]}{K_{D1}} + 1 \quad (3)$$

They obtained K_D values that compared reasonably well to solution-phase data. However, very high charge states of BSA were observed, a possible indication of partial denaturation. Eckart and Spiess [74] used ESI–MS to monitor the concentration dependent binding of biotin to streptavidin, and found a saturation of streptavidin with biotin at a concentration corresponding to the expected binding capacity. A study dealing with the binding of various peptides to SH2 motifs, which are important in signal transduction and antigen receptors was carried out by Loo et al. using ESI–MS [75]. Phosphorylated and unphosphorylated peptides were examined. Only the phosphorylated peptides were found to bind to the SH2 domain, as expected from solution-phase results. From titration curves, Scatchard plots similar to those used by Greig et al. [72] and Lim et al. [71] were constructed. The results were in reasonable agreement with IC_{50} values obtained in solution and with literature values. IC_{50} is the concentration of the inhibitor needed to reduce the specific binding of the inhibitor to the enzyme to 50%.

A more complex system was investigated by Ayed et al. [76]: citrate synthase (CS) from *Escherichia coli* was titrated with its allosteric inhibitor NADH. In a first step, the association constant K_A of the dimer to hexamer was determined by varying the subunit concentration of CS (Fig. 4). Assuming a simple equilibrium between dimers and hexamers, K_A was determined to be $6.9 \times 10^{10}\,M^{-2}$. This is the only study where differences ionization efficiency were explicitly taken into account.

In the same study, the K_D for NADH binding to the dimer or the hexamer was determined by titrating a fixed concentration of protein with increasing concentrations of NADH. Different binding sites could be distinguished: a relatively loose binding site per subunit for the dimer ($K_D = 28.3\,\mu M$), one tight binding

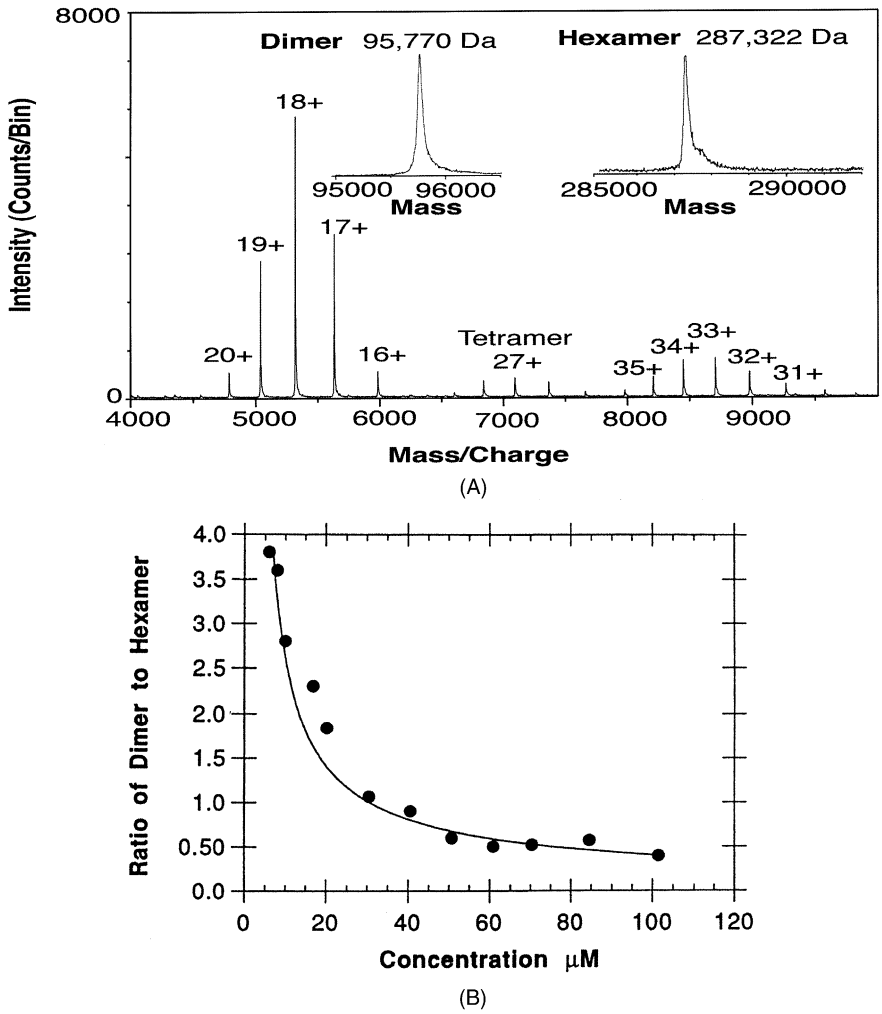

Fig. 4. (A) ESI-TOF spectrum of citrate synthase (9 μM subunit concentration) in 5 mM ammonium bicarbonate buffer at pH = 7.5. Deconvolutions of the regions corresponding to the dimer and the hexamer are shown as insets. A 300 V declustering voltage was used to obtain this spectrum. (B) Dependence of the dimer/hexamer molar concentration [D]/[H] on the citrate synthase subunit concentration. The integrated peak areas were corrected for the different transfer coefficients, as described in the text. From a fit of the data (solid line) a dimer–hexamer association constant $K_A = [D]/[H] = (6.9 \pm 0.7) \times 10^{10}\,M^{-2}$ is obtained. From [76], © John Wiley & Sons Ltd., reproduced with permission.

site per subunit for the hexamer ($K_D = 1.1\,\mu M$) and two loose binding sites per subunit for the hexamer with a K_D of about 150 μM. In addition, binding of NADH shifted the equilibrium between dimer and hexamer to the hexamer, which could be shown for the first time with these mass spectrometry results.

Similar studies have been published by Griffey et al. [77], Sannes-Lowery et al. [73], and Carte et al. [78]. The paper by Sannes-Lowery et al. [73] is interesting because different methods were tested for obtaining dissociation constants of RNA–aminoglycoside complexes, e.g., keeping the RNA concentration constant and titrating with aminoglycoside, or fixing the aminoglycoside concentration and titrating with RNA. This comparison yielded different results, and the authors came to the conclusion that the best method is holding the RNA concentration constant below the expected K_D and titrate with the ligand. This, however, shows that K_D values determined by titration for an unknown system have to be treated with caution.

3.1.3. Determination of transfer coefficients

Mass spectral peak intensities are often taken as a direct measure of solution-phase concentrations. However, does the mass spectrum reflect the solution-phase concentrations of the different species? This is a key question, and depends on relative vaporization and ionization efficiencies of different molecular species. For a compound X, a transfer coefficient t_X can be defined that accounts for all instrumental and chemical effects that decrease or enhance the mass spectrometric signal for compound X, $I_X = t_X[X]$. Very few studies address this problem explicitly. Rather, similar transfer coefficients for the free host and the host–guest complex are implicitly assumed, in particular for systems where the guest is much smaller than the host. As discussed later, this assumption is not generally fulfilled.

Johnstone and coworkers [24,25] employed a correction procedure for taking into account the varying FAB–MS sensitivities towards different noncovalent complexes. The study of Leize et al. [63] deals with the reasons for different ionization efficiencies. They found the solvation energy of different species to be the key parameter for relative quantification by ESI–MS. For example, an equimolar mixture of LiCl, NaCl, KCl, RbCl and CsCl yields very different relative intensities in the mass spectrum, with Cs^+ being the most intense and Li^+ being the least intense peak with only 2% intensity compared to Cs^+. The response factor of the metal ion M, k_M, was found to depend exponentially on the solvation energy E_M of this ion, $k_M = C\exp(-0.015E_M)$, where C is a constant depending on the ion charge, the ion concentration and the instrument parameters. In contrast to this, spectra of equimolar mixtures of three or four of these cations in the presence of the same amount of the crown ether cryptate 222 showed peak intensities that reflect the proportions calculated from well known solution-phase stability constants. The authors explain this with the similar solvation energies of the crown ether complexes, in contrast to those of the alkali cations, which are very different. This thus seems to argue for the use of uniform transfer coefficients.

Young et al. [79] also addressed the question of different transfer coefficients in titration type experiments using crown ethers. The molar ratio of two salts, e.g., LiCl and KCl was varied from 1:1 to 5:1 and to these solutions an excess of crown ether was added such that all alkali ions were complexed. Then the ratio of peak intensities of K^+ and Li^+ was plotted against the ratio of concentrations, yielding a linear relationship with a slope that equals the ratio of the transfer coefficients. The transfer coefficients of the Li^+–crown ether complex was only 0.532 of that of the K^+–crown ether complex. This is in contrast to the study of Leize et al. [63], where the peak intensities of crown ethers complexed with different metal ions were found to reflect the expected solution-phase concentrations. Dubois et al. [80] presented a MALDI study of alkali–crown ether complexes, using a special particle/liquid matrix mixture, with glycerol as the liquid matrix. They first determined the transfer coefficients relative to the Cs^+–crown complex, and were able to determine relative stability constants based on this calibration. Good agreement with results from an earlier EHMS study [27] that had used glycerol as the liquid medium was found. Some of the transfer coefficients reported by

Dubois et al. [80] differed by a factor of 5.3, although the same crown ether was used for all complexes. In the paper of Ayed et al. [76] the authors take the different response factors of citrate synthase dimer and citrate synthase hexamer into account. They calibrate their measurements by measuring a known concentration of pure hexamer and of a specially modified dimer that will not form hexamers. Based on this calibration, peak intensities can be converted to concentrations of dimer or hexamer. This revealed a sensitivity ratio of 1.3, which means that an equimolar mixture of dimers and hexamers would give a peak area ratio of 1.3. These three studies clearly show the importance of taking ionization efficiencies into account. In many cases, they will significantly affect the determination of association constants by mass spectrometric methods.

3.1.4. Competition methods

The term "competition methods" indicates that different host–guest complexes are measured simultaneously. One can either use different hosts competing for one guest, or one host and different guests competing for the binding site. Information about the absolute binding affinities, relative binding affinities, or selectivity of the different guests or hosts can be obtained. It is possible to obtain either relative or absolute binding affinities.

An interesting technique to determine absolute binding constants of different guests to one host was published by Jørgensen et al. [81]. These authors determined the binding constants of a number of guest molecules with vancomycin and risocetin; all were found to be in good agreement with literature values. Fig. 5 shows a measurement of the binding constants of vancomycin with three peptide guests in a single ESI–MS experiment.

The method is based on the measurement of the relative peak intensities of the free host (vancomycin) and the three complexes of the host with three different guests. In solution the equilibrium concentration of the host and the three complexes is given by

$$[\mathrm{H}_i] = \frac{\mathrm{H}_i[\mathrm{H}_i]_0}{\mathrm{H} + \mathrm{HG}_1 + \mathrm{HG}_2 + \mathrm{HG}_3} \tag{4}$$

where H, HG_1, HG_2 and HG_3 are the peak intensities of the host and its three complexes with the different guests, the square brackets denote concentrations, $[H_i]_0$ is the initial concentration of host, and H_i refers to any form of the host. For an equimolar mixture the binding constant for complex HG_1 can be expressed as follows:

$$K_{\mathrm{HG}_1} = \frac{[\mathrm{HG}_1]}{[\mathrm{H}][\mathrm{G}_1]} = \frac{[\mathrm{HG}_1]}{[\mathrm{H}]([\mathrm{H}] + [\mathrm{HG}_2] + [\mathrm{HG}_3])} \tag{5}$$

Note that this equation only holds if equimolar solutions are being used. The major advantage of this method is its speed. Within seconds one can determine the binding constant of several noncovalent complexes at once. A key assumption in this method is that the ionization efficiencies of the host and the complexes are identical. This can only be expected if the host is much heavier than the guest compounds and thus determines the ionization efficiency. A different method for determination of absolute binding constants of mixtures has also been published by Jørgensen et al. [82].

Kempen and Brodbelt recently published a very useful competition method to determine absolute binding constants by ESI–MS [83]. The same method has already been used by Gokel et al. to determine binding constants of Ca^{2+}–crown ether complexes using ion selective electrodes [84] and by Goff et al. to determine the binding constants of Rb^{+}–crown ethers by NMR [85]. The binding constant of a complex is determined indirectly, by following only the signal of a reference complex with known binding constant. The reference complex must either contain the same guest or the same host as the complex under investigation. The first step is to acquire a calibration curve for the reference complex. The concentration of the reference complex $[H_RG]$ can be calculated for each calibration point (Eqs. (6)–(8)):

$$K_{\mathrm{R}} = \frac{[\mathrm{H_R G}]}{[\mathrm{H_R}]_{\mathrm{F}}[\mathrm{G}]_{\mathrm{F}}} \tag{6}$$

$$[\mathrm{H_R}]_{\mathrm{F}} = [\mathrm{H_R}]_{\mathrm{T}} - [\mathrm{H_R G}] \tag{7}$$

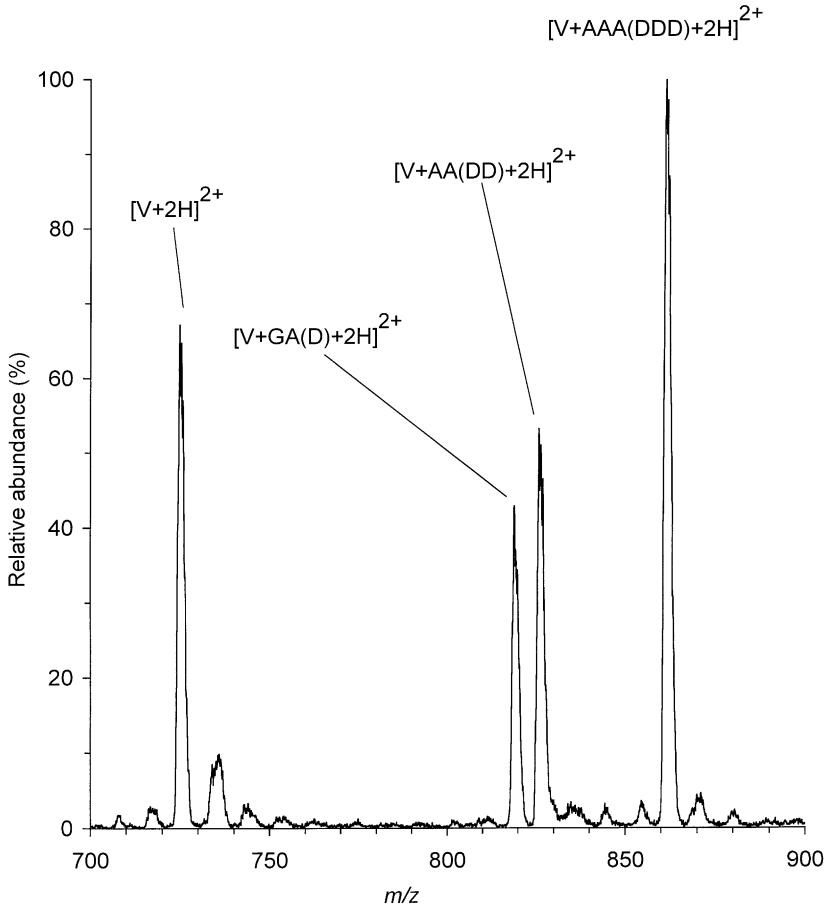

Fig. 5. Partial ESI mass spectrum obtained for an equimolar (50 mM) mixture of vancomycin (V), acetyl-D-Alanyl-D-Alanyl-D-alanine (AAA(DDD)), acetyl-D-Alanyl-D-alanine (AA(DD)) and acetyl-glycyl-D-alanine (GA(D)) in 5 mM ammonium acetate buffer at pH 5.1. Reprinted with permission from [81]. Copyright 1998, American Chemical Society.

$$[G]_F = [R]_T - [H_RG] \quad (8)$$

where index R stands for reference complex, index T for the total amount of guest (G) or host (H) and index F for free guest or host. The second step is the actual competition experiment. A spectrum from a solution containing the reference complex and the unknown complex is recorded, but only the concentration of the reference complex is observed and determined with help of the calibration curve. From the concentration of the reference complex in the competition experiment, the binding constant of the unknown complex can be calculated. For the equilibrium in the competition experiment the following equations are used:

$$K_R = \frac{[H_RG]}{[H_R]_F[G]_F} \quad (9)$$

$$K_N = \frac{[H_NG]}{[H_N]_F[G]_F} \quad (10)$$

$$[G]_F = [G]_T - [H_RG] - [H_NG] \quad (11)$$

$$[H_R]_F = [H_R]_T - [H_RG] \quad (12)$$

$$[H_N]_F = [H_N]_T - [H_NG] \quad (13)$$

where G is the guest which is the same for the known and unknown complex. H_R is the reference host and

H_N is the host of the unknown complex. By solving these five equations simultaneously one can obtain the binding constant of the unknown complex (Eq. (14)):

$$K_N = \left[\frac{[H_RG] + K_R([H_R]_T - [H_RG])([H_RG] - [G]_T)}{-[H_RG] + K_R([H_N]_T + [H_RG] - [G]_T)([H_RG] - [H_R]_T)}\right]\left[\frac{K_R([H_R]_T - [H_RG])}{[H_RG]}\right] \quad (14)$$

Stable spray conditions must be found for obtaining a useful calibration curve for the reference complex, and the stability of the spray must persist during the competition experiment. For proteins this is sometimes difficult. Furthermore, the method assumes that the ionization efficiency of the reference complex is constant during the whole measurement, i.e., that the presence of the unknown substance (guest or host) does not influence the ionization efficiency of the reference complex. This may not always be the case. The greatest advantage of this method is that the ionization efficiency of the unknown complex does not matter and thus no transfer coefficient needs to be estimated. For example, even if one of the species cannot be ionized (i.e., ionization efficiency = 0), it is still possible to determine the binding constants. Once the calibration curve has been established, the method is very fast, which is, for example, advantageous for screening a library of guests for the same host. For reference and unknown complexes where the K_A differs by up to two orders of magnitude, a 1:1:1 concentration ratio can be used in the competition studies. If the K_A value differs by more than that, the concentration ratio has to be adjusted. Kempen has validated this method using different crown ether hosts with potassium as the guest, and very good agreement with solution-phase association constants was found.

Relative binding affinities or selectivities can also be determined with competition methods. Experiments and validation studies with different crown ethers, their analogons, and cryptants [23,63,86–100], with self-assembling hosts [101], with single and double stranded oligonucleotides [64,102–108] and with different proteins [19,65,66,75,109] have been described in the literature.

Cheng et al. used ESI–FT-ICR–MS to determine the relative binding affinities of 16 inhibitors derived from *para*-substituted benzenesulfonamides to bovine carbonic anhydrase II (BCA II, 29 kDa) in a single competition experiment [110]. They found that the relative abundances of the complex ions were consistent with the binding constants of the inhibitors in solution. For control experiments they prepared a four-component mixture of inhibitors with their concentrations inversely proportional to their K_A values. The inhibitors formed 1:1 complexes with BCA II, with approximately equal ion abundances, as expected. They also carried out two control experiments to assure that the noncovalent complexes are specific. For the determination of complexes with nearly equal mass they carried out tandem mass spectrometric experiments. The relative intensities of the inhibitors were similar to those obtained from spectra of the intact complexes and correlated with the relative binding affinities in solution. For structural identification of the inhibitors they performed MS^3 experiments leading to distinctive fragmentation patterns indicative for the structure of the compounds. In their experiments, they showed very carefully that the ESI–MS method is suited for the determination of the selectivity.

Goolsby et al. [111] published an interesting article about the determination of alkali ion binding selectivities of calixarenes by MALDI and ESI quadrupole mass spectrometry. Because MALDI is rarely used for this kind of work and because the authors compare the results obtained by MALDI and by ESI, this article deserves some special attention. The results show some moderate differences in the specific ratio of K^+ complexes to Na^+ complexes in the MALDI vs. the ESI spectra for each calixarene, but preferences towards K^+ or Na^+ for the various calixarene are consistent. The evaporation of solvent to dryness may exert some influence on the selectivity derived by MALDI–MS. A problem was the alkali ion contamination of the MALDI matrices, and the large shot-to-shot fluctuations.

3.2. Gas-phase methods

Most ESI–MS studies suggest that important structural features of large biomolecular assemblies are retained in the gas phase; even for MALDI this has been found to be the case under certain conditions. On the other hand, biomolecules are desolvated upon transfer into the vacuum of the mass spectrometer. This implies that electrostatic interactions and hydrogen bonds, that surely survive the spray process, are largely responsible for maintaining structural features of the vaporized biomolecular ions. Hydrophobic interactions are believed to be partly or completely lost in the gas phase [65,112]. In general, therefore, no correlation between the gas-phase stability and the solution-phase stability of noncovalent complexes can be expected. Results from most of the studies support this conclusion. However, there are some exceptions, cases, in which it has to be assumed that the dominant interactions are very similar in the gas phase and in solution, and that solvent mediation or screening plays a minor role.

3.2.1. Cone voltage-driven dissociation (VC_{50} method)

Dissociation induced by increasing the cone voltage (VC) of the ions in the source–analyzer interface region of an ESI mass spectrometer is a rapid and fairly straightforward method for evaluating relative gas-phase stabilities. This voltage determines the kinetic energy acquired by the noncovalent assembly, and thus the excitation when it collides with other gaseous molecules. The dissociation of the chaperone GimC/prefolding homologue complex has been studied with this method [70]. The experiments revealed a quaternary arrangement of two central and four peripheral subunits. Increasing VC from 50 to 150 V led to a disruption of the hexamer and the observation of a pentameric species. This loss of a single (monomeric) unit as an initial dissociation step suggested that these subunits were located at peripheral positions of the larger assembly, thereby facilitating their successive release as the collision energy was increased.

The VC value needed to dissociate 50% of a noncovalent complex initially present (VC_{50}) is taken as a gas-phase stability parameter, e.g., of an enzyme–inhibitor complex. This method has been utilized by Rogniaux et al. in a very nice study: their methodology allows to rapidly supply information about how inhibitors interact with their target enzyme [113]. Fig. 6 exemplifies how the VC_{50} value correlates with the energy of the electrostatic and hydrogen bond interactions of the aldose reductase inhibitor noncovalent complex. The ESI mass spectra of an equimolar mixture of aldose reductase, coenzyme ($NADP^+$) and its inhibitor LCB3071 are recorded at various cone voltages.

The extent of ternary complex dissociation is visualized through the appearance of the holo-enzyme species (without inhibitor), as the cone voltage is increased from 65 to 95 V. For each VC value, this extent may be calculated by measuring the abundance of the holo-enzyme, relative to that of the complexed species. Measuring the VC_{50} values for different inhibitors, the relative order of gas-phase stabilities was compared to relative interaction energies obtained from X-ray crystallography data. Rogniaux et al. [113] report a clear qualitative correlation between the calculated binding energies and the gas-phase stabilities evaluated by the VC_{50} method. However, no quantitative correlation was found, as the investigated protein may be partially denatured during the MS experiment. The authors point out the striking fact that solution-phase parameters (IC_{50} values), giving key information about the inhibition level of a drug, do *not* follow the order of VC_{50} (=gas phase) values of aldose reductase–inhibitor complexes. Similar conclusions have been drawn by other groups, for example when studying dissociation of heme from myoglobin and cytochrome *b5* [114] or for the dissociation of oligodeoxynucleotide duplexes [115].

3.2.2. Collision-induced dissociation (CID)

CID is used to induce unimolecular decay of mass selected ions with sufficient internal energy upon activation by collision with a neutral gas [116]. The center-of-mass energy for a single collision is given by $E_{com} = E_0[m_t/(m_t + m_p)]$ where E_0 is the laboratory frame kinetic energy, m_t the mass of the target

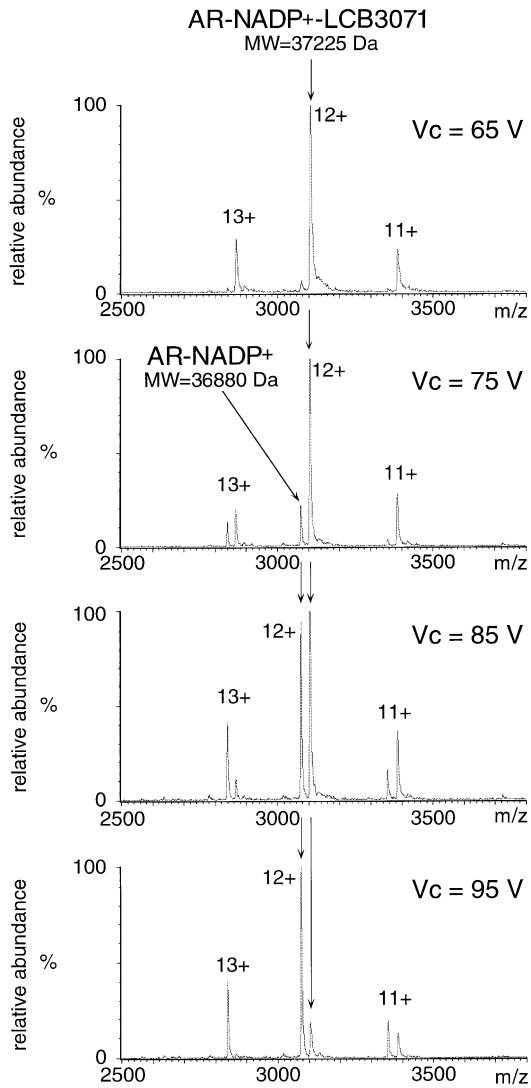

Fig. 6. Gas-phase stability study of the enzyme–coenzyme–inhibitor complex aldose reductase–NADP(H)–LCB3071. The ternary complex gradually dissociates in the gas phase when the cone voltage VC_{50} is increased. Spectra were recorded for four different VC_{50} values, 65, 75, 85, and 95 V. The pressure in the source–analyzer interface was kept constant at 2 mbar. Spectra were not corrected for different ionization efficiencies of different compounds, but different responses in ESI analysis have been shown to be irrelevant for the aldose reductase example. Reproduced with permission of Elsevier Science from [113]. Copyright 1999, by the American Society for Mass Spectrometry.

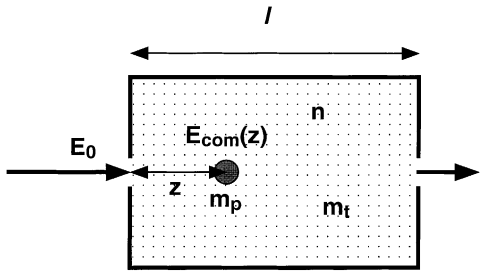

Fig. 7. Schematic of a CID collision cell. E_0 is the laboratory frame kinetic energy of the ion injected into the collision cell, $E_{com}(z)$ is the center of mass collision energy after passing a distance z into the collision cell, m_t is the mass of the target gas and m_p the mass of the complex ion, n the gas number density, and l is the overall length.

gas and m_p is the mass of the complex ion. The total energy transferred to the ions is the fraction of internal energy transferred as the ion travels an incremental distance δl, integrated over the entire length of the collision cell (Fig. 7).

The internal energy acquired by the ions passing through a CID collision cell, E_{int}, is calculated using the following equation:

$$E_{int} = \frac{m_t}{M}\phi\frac{m_p E_0}{m_t C_D}\{1 - \exp(-C_D n m_t \sigma l/m_p)\} \quad (15)$$

where $M = m_p + m_t$, ϕ the average fraction of center-of-mass energy transferred to internal energy of the ion in a collision, C_D the drag coefficient, n the gas number density, σ the collision cross-section, and l is the length of the collision cell [117]. This expression accounts for energy loss as the ions pass through the collision cell and also corrects for the greater number of collisions of ions with larger cross-sections. For a small exponent and $\phi = 1$, Eq. (15) reduces to

$$E_{int} = \frac{E_0 n \sigma l m_p}{m_t + m_p}. \quad (16)$$

This energy transfer is thus influenced by the collision gas pressure, the molecular weight of the collision gas, the cross-section of the ions, the injection energy of the ions, and the loss of kinetic energy as they pass through the collision cell. Due to Coulombic repulsion, higher charge state ions have higher collision cross-sections; they also experience greater acceleration

than ions with lower charge states. Hence, ions bearing more charges collide with more energy, leading to a faster increase in internal energy.

Using ESI–MS/MS, Li et al. [66] compared the relative binding energies of rapamycin and four of its analogs to the cytoplasmic receptor FKBP. They concluded that the gas-phase binding reflects the aqueous solution behavior in these complexes. Penn et al. [118] studied CID of complexes of peptides with cyclodextrin. Ions were produced by electrospray ionization (ESI–FT-ICR). Trapped ions were excited with an RF pulse and allowed to undergo CID in the analyzer cell, using N_2 as collision gas. In an FT-ICR experiment, the laboratory frame kinetic energy E_0 can be calculated in the following way:

$$E_0 = \frac{z^2 B_0^2 r^2}{2m} \tag{17}$$

where m is the mass and z the charge of the ion, B_0 the magnetic field strength, and r is the cyclotron radius after ion excitation ($r = \beta V t_{ex}/2B_0$, where V is the peak-to-peak excitation amplitude, t_{ex} the duration of excitation pulse, and β is the geometry factor of the FT-ICR cell). In this study, the threshold of fragmentation was defined as the bottom-to-peak voltage ($V_{b–p}$) at which fragments are first observed with a 2% relative intensity. This is determined from a plot of percent dissociation of the complex vs. amplitude of applied radio frequency. Threshold values $V_{b–p}$, E_0, E_{com}, and E, the total energy transfer in an infinite number of collisions were calculated and compared with dissociation temperatures obtained using heated capillary dissociation method. The threshold values measured by CID for four related complexes were found to follow the same order observed in heated capillary dissociation method. However, E-values obtained for infinite collision conditions are found to be very large compared to the expected binding energy values. Hence, this method can be used for the comparison of related systems for the threshold values rather than for the determination of absolute value for the binding energies.

Chen et al. [117] have used tandem mass spectrometry and ion trapping experiments to study the heme binding in holo-myoglobin. They have shown that the energies required to dissociate heme from the highly charged heme–protein complex in the gas phase are similar to those of low charge states indicating that heme–protein interactions remain relatively unperturbed in the partially unfolded highly charged ions. In tandem mass spectrometry, the dissociation voltages giving 50% apo-myoglobin (aMb) from holo-myoglobin (hMb) are obtained from the plots of injection voltage vs. relative intensity of the aMb signal. Complexes with charges from +8 to +19 were studied at different collision cell pressures. The heme binding energy was calculated using the collision model. For the charges from +9 to +12 charge states the calculated energies were very similar. The authors also carried out ion trapping experiments and compared these results with the tandem MS results. They showed that the highly charged hMb can be trapped for a period of 0.5 s without loss of heme. The rates for the loss of hMb were measured and activation energies were calculated from the Arrhenius equation. Calculated activation energies were found to correlate well with the relative binding energy calculated in the MS/MS experiment and also showed that the binding energies of heme in high charge states of hMb are similar to those of low charge states. Related work on hemoglobin has also been presented by Apostol [119].

Jørgensen et al. [120] studied molecular recognition in the gas phase using CID in a triple quadrupole mass spectrometer. Noncovalent complexes between vancomycin antibiotics and peptide ligand stereoisomers were studied and compared with solution-phase binding studies. This is the same system as studied earlier by Lim et al. [71] described in Section 3.1.2. Dissociation efficiency curves (plots of percent dissociation vs. center-of-mass collision energy under single collision conditions) were used to find the threshold CID energy. The order of gas-phase stability for the negatively charged vancomycin–peptide complexes was found to be identical to the order of solution association constants, indicating that the structural features responsible for the stereoselective binding of these peptides are preserved in the gas-phase anionic complexes. Interestingly, the corresponding positively charged complexes did not reflect the solution state behavior. This

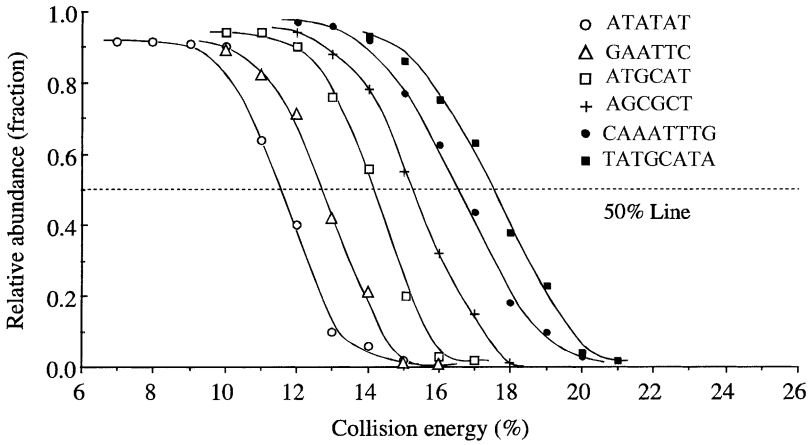

Fig. 8. Dissociation profiles of DNA duplexes, 6-mers and 8-mers (−3 charge state). Reproduced with permission of Elsevier Science from [122]. Copyright 2000, by the American Society for Mass Spectrometry [122].

was attributed to the destruction of the specific interaction between the antibiotic and the peptide in the protonated complex. Heck and coworkers [121] used CID to study a similar system, the noncovalent complexes of an antibiotic, avoparcin, with bacterial cell wall precursor peptides. They reported that the order of gas-phase stability of the protonated complexes (positive ions) is different from the order of stability of the same complexes in solution. The authors further concluded that the doubly protonated complexes are not the same as those formed in solution.

Wan et al. [122] have used CID in an ion trap mass spectrometer to study the various factors influencing the stability of nucleotide duplex–drug complexes. Analogous to a VC_{50} value, a collision energy E_{50} for 50% dissociation of the complex was used as a measure of complex stability. The effect of number of charge, number of base pairs, location of the high proton affinity base pair and the number of hydrogen bonds on the stability of duplex was studied (see Fig. 8).

When the charge states are identical, the stability is proportional to the number of hydrogen bonds in the duplex, correlating well with solution-phase measurements (Fig. 9). The stability of noncovalent complexes between duplex oligonucleotides and drug molecules were also studied. By comparing the E_{50} values, the relative stability of the complexes and the mode of binding of the drug molecules were compared. The dissociation of the duplex bound to the drug results in two single strands, one with the drug and one without the drug. Using E_{50} values, it was even possible

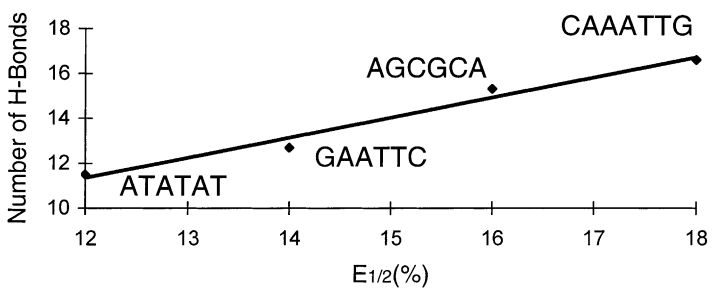

Fig. 9. Correlation of measured E_{50} values with the number of H bonds in some of the duplexes shown in Fig. 8. Reproduced with permission from [122]. Copyright 2000, American Society for Mass Spectrometry [122].

to differentiate between drugs that are binding to the minor grooves and others that intercalate.

Smith and coworkers [29,112,123] studied noncovalent complexes between BCA II and substituted benzenesulfonamide inhibitors in the gas phase and solution phase. The same system was previously investigated by a mass spectrometrically detected competition experiment in solution [110] as described in Section 3.1.4; agreement with known solution-phase association constants was found. Wu et al. [112] found that the gas-phase stability of the complexes increases with the polar surface area of the inhibitor indicating the dominant role of polar surface interactions in the gas phase. In contrast, Gao et al. [123] used structural isomers of benzenesulfonamide as ligands, which have the same polar surface area. They showed that the specific interaction between the inhibitor's sulfonamide group and Zn(II) ion on carbonic anhydrase is retained in the gas-phase complex. They also studied the steric interaction of the inhibitor with the binding pocket and concluded that carbonic anhydrase retains, at least partially, the structure of its binding pocket in the gas phase on the time scale of seconds to minutes.

Nesatyy [124] has investigated the gas-phase binding of noncovalent protein complexes between bovine pancreatic trypsin inhibitor (BPTI) and its target enzymes (trypsin, chymotrypsin, trypsinogen) by CID tandem mass spectrometry/ESI–MS/MS. V_{50}, defined here as the voltage difference between sections Q_0 and Q_2 of a triple quadrupole mass spectrometer, was calculated from the dissociation curves and used for the internal energy calculations. Collision cross-sections for these ions were determined using energy loss measurements. Various factors influencing complex dissociation in the gas phase, such as the difference between orifice and skimmer potentials, the charge state of the ion, nature of the collision gas and its pressure were studied, as shown in Fig. 10.

V_{50} values for complexes between BPTI and its target enzymes showed significant variation and did not correlate well with their solution analogs. The relative internal energy required to dissociate 50% of the complexes is in the order chymotrypsin–BPTI > trypsinogen–BPTI > trypsin–BPTI. In solution the order is trypsin–BPTI > chymotrypsin–BPTI > trypsinogen–BPTI. The nature of interactions in these complexes is different and the desolvation processes taking place in the formation of gas-phase ions affect these interactions differently in different complexes, i.e., the ratio between the hydrophobic and the polar interactions determines the stability of the gas-phase complex.

3.2.3. Guided ion beam tandem mass spectrometry

The CID process can be examined by any tandem mass spectrometer. However, the need to accurately measure the absolute energy for threshold dissociation requires more rigorous experimental methods such as guided ion beam mass spectrometry (GIBMS). Qualitatively, the greatest emphasis in GIBMS instrumentation is put on designing the reaction zone for dissociation, rather than on mass selective parts. GIBMS as well as the theory to evaluate the experimental data has been largely developed by Armentrout and coworkers [125–129].

Guided ion beam mass spectrometry has been applied to noncovalent complexes [33,130], albeit this research has largely been limited to the study of metal ion–ligand complexes, with ligands such as water, small alcohols and ethers, crown ethers, and a handful of small heteroaromatic ligands. The topic is thus not within the scope of this review. Flowing afterglow ion sources have been used most frequently in GIBMS, because internal and kinetic energies of the ions produced are easily characterized and controlled. This is a critical aspect for obtaining accurate data from such experiments. Soft ionization methods have not generally been well characterized with regard to the true temperature of the ions. However, progress is being made [131,132], and we hope that larger noncovalent complexes will soon become accessible for investigation by guided ion beam-threshold dissociation methods.

3.2.4. Blackbody infrared radiative dissociation (BIRD)

BIRD is an interesting method that has been introduced by Dunbar and McMahon [133], and

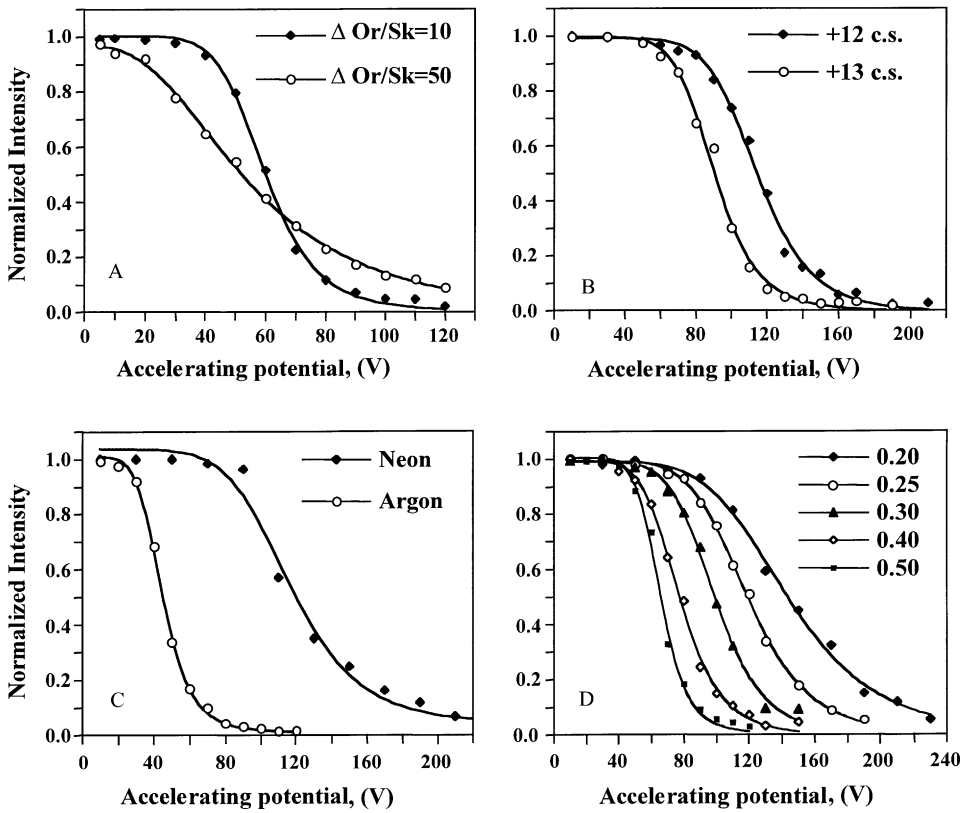

Fig. 10. Factors affecting the dissociation of the trypsin–bovine pancreatic trypsine inhibitor (BPTI) noncovalent complexes in the gas phase. The *y*-axis shows the fraction of intact complex. (A) Effect of the orifice–skimmer voltage (VC, indicated as Or/Sk (V)); 0.5 mTorr of Kr gas, +12 charge state; (B) effect of the charge state at 1.4 mTorr of Ne; (C) effect of the nature of the collision gas on the dissociation of the +13 charge state at 1.2 mTorr gas pressure; (D) effect of the collision gas pressure (Kr, mTorr) on the dissociation of the +12 charge state. From [124], © John Wiley & Sons Ltd., reproduced with permission.

was more recently extended for the study of large molecules [134,135], including noncovalent complexes [136–139]. In this method, the blackbody radiation of the heated vacuum chamber walls is employed to dissociate trapped ions. Strictly speaking, only unimolecular dissociation is probed by BIRD. However, the rate of energy exchange between the trapped ions and the chamber walls can greatly exceed the dissociation rate such that the trapped ions have a Boltzmann distribution of internal energy characterized by a temperature. From the temperature dependence of the dissociation rate, activation energies and pre-exponential factors can be determined from an Arrhenius plot. Direct information on the relative thermal stability is thus available, and in the absence of a reverse barrier, the activation energy reflects a threshold dissociation energy. Using the BIRD method, Gross et al. [136] determined the gas-phase dissociation rate of heme from holo-myoglobin to be considerably lower than from holo-hemoglobin α-chain, and somewhat dependent on solution pH and on the ion charge state studied. The dissociation activation energies of double strand oligonucleotides were also studied by BIRD [137,138], and found to range from 1.2 to 1.7 eV, depending on the number of nucleobases present and the degree of complementarity. Based on four lines of evidence, it was concluded that Watson–Crick base pairing is preserved

in the gas phase, i.e., in the absence of solvent. For complementary duplexes, the gas-phase activation energies correlated well with solution binding free energies. Strittmatter et al. [139] went one step further and used master equation modeling of BIRD data of nucleotide dimers in order to obtain threshold dissociation energies. The dissociation energy for the guanosine monophosphate–cytosine monophosphate dimer anion was found to be higher than for any other nucleotide dimer, again consistent with a Watson–Crick type hydrogen bonding.

Price et al. [140] used BIRD to determine the nature of proton-bound dimers of betaine and of betaine with protonated bases of similar gas-phase basicities. These authors attributed some of the higher binding energies measured to the existence of ion–zwitterion structures in the gas phase.

Klassen and coworkers have conducted a couple of BIRD studies on the pentamer of Shiga-like toxin I (B_5) and its complexes with oligosaccharide ligands [141,142]. The magnitude of the Arrhenius parameters for dissociation of the pentamer and the B_5–ligand complexes were found to be highly charge dependent. In the dissociation of the complexes, the loss of a ligand was found to compete with loss of a B subunit at low temperature. The pentamer itself was found to dissociate almost exclusively by the loss of a single subunit B, carrying a disproportionally large fraction of the parent ion charge, up to 50%. This was compared to the asymmetric dissociation process in droplet fission in electrospray ionization, where smaller offspring droplets are believed to form with much higher m/z than the parent droplet. Finally, excellent agreement was found between the complex binding affinity determined from ion intensities of complexed and free B_5 in the ESI mass spectrum and the binding affinity derived from microcalorimetry [142].

3.2.5. Heated capillary disociation (thermal dissociation in the gas phase)

A heated transfer capillary consisting of two independently heated segment can be used to dissociate noncovalent complexes. The complex is first desolvated in the first segment and then dissociated in the second segment (see Fig. 1). Under these conditions thermal dissociation of the complex takes place in the gas phase. A stable temperature range of the first segment of the capillary where desolvation is complete but no dissociation occurs is first established. Dissociation of the complex is then performed by systematically raising the temperature of the second segment.

Lebrilla and coworkers [143,144] studied heated capillary dissociation (HCD) of cyclodextrin inclusion complexes using this approach in an FT-ICR–MS. HCD graphs were obtained by plotting the normalized intensity of the complex vs. temperature of segment 2. In the work by He et al. [143], the dissociation temperature T_D was arbitrarily defined as the temperature at which the complex intensity falls below 1% of the most abundant peak. T_D values for the complexes of bradykinin and three of its analogs with cyclodextrin were compared. The relative order was shown to correlate well with CID threshold energies for these complexes. The apparent activation energy for dissociation and the apparent pre-exponential factor could also be determined from an Arrhenius plot. The uncertainties in the measurement of temperature and the complexity of the dissociation processes limits the utility of this method for determining absolute activation energies and pre-exponential factors. Comparison of the E_a(HCD) and A(HCD) with the values obtained for the same complexes using BIRD shows that the values obtained by HCD are higher. This method could be used for comparison of similar systems using T_D. Garcia et al. studied HCD of protonated cyclodextrin–amino acid complexes [144]. T_D of the complexes were shown to increase with the number of hydrogen bonds and the ability of the cyclodextrin host to sterically lock the amino acid guest in place.

3.2.6. Other gas-phase methods

Numerous methods have been described in the literature for measuring binding enthalpies and free energies of gas-phase complexes, for example, equilibrium methods for determining metal ion affinities to various ligands [145,146], photodissociation methods [147–151], and Cooks' kinetic method [152–154].

A large body of literature also exists on high pressure mass spectrometry methods used for the determination of equilibrium constants and ligand binding energies of noncovalent complexes [155–161]. With very few exceptions, binding of small molecular ligands (H_2, H_2O, NH_3, simple amines, simple hydrocarbons, etc.) to metal ions have been studied, a subject that we have decided to exclude in this review. Recently, somewhat larger ligands have been investigated, for example amino acids and small peptides [162–164], oligonucleotides [165], and substances used as MALDI matrices [166]. An interesting approach that is complementary to gas-phase dissociation methods is to monitor gas-phase complex *formation* by the so-called radiative association process where the initial metastable complex is stabilized by photon emission [167]. The kinetics of complex formation in low pressure FT-ICR experiments, where radiative stabilization dominates over collisional stabilization have been analyzed in order to obtain quantitative values for the complex binding energies. High precision values are available from fitting the experimental data, using an expression that contains the binding energy as a fit parameter. Again, this method has not been applied to high molecular weight complexes produced by ESI or MALDI, but rather to complexes between metal ions and small organic ligands [167]; the highest molecular weight ligands studied so far were phenol, indole, and coronene [168,169].

4. Measurements of stereoselectivity by MS

Soft ionization mass spectrometry has been used quite frequently to determine stereochemical properties of chiral compounds [170]. These studies involve the formation of diastereomeric noncovalent complexes between a chiral selector C and the chiral molecule. The stereoselectivity is obtained by quantitative determination of the kinetics or thermodynamics associated with the dissociation of this complex (Eq. (18)), or from measuring the rate of guest exchange equilibria in the gas phase. This topic is thus closely connected with the subject of this review

$$(\text{products})_S \overset{k_S}{\leftarrow} [CS] \underset{+S}{\overset{\kappa_S}{\rightleftharpoons}} C \underset{-R}{\overset{\kappa_R}{\rightleftharpoons}} [CR] \overset{k_R}{\rightarrow} (\text{products})_R \tag{18}$$

Fast atom bombardment mass spectrometry has also been used to study chiral recognition between small organic molecules, as reviewed by Sawada [171]. Yao et al. have reported the chiral analysis of 19 common amino acids using ESI–MS/MS [172]. CID of protonated dimers, trimers and tetramers formed between the chiral selector and the amino acid was used to find the chiral recognition ratio (CR). If we consider the following reaction:

$$XY_nH^+ \rightarrow XY_{n-1}H^+ + Y \tag{19}$$

where X is the amino acid, Y the chiral selector, and $n = 1, \ldots, 3$, CR is defined as

$$CR = \frac{([XY_{n-1}H^+]/[XY_nH^+])_{LD} + ([XY_{n-1}H^+]/[XY_nH^+])_{DL}}{([XY_{n-1}H^+]/[XY_nH^+])_{LL} + ([XY_{n-1}H^+]/[XY_nH^+])_{DD}} \tag{20}$$

For each complex ion, all four chiral combinations of the chiral selector and the amino acid were studied. This method was shown to work well for the determination of the chirality of an amino acid in a mixture. The same group has applied a MS technique to find the enantiomeric excess in amino acids [173]. Collision-induced dissociation of the trimers formed between the amino acids and the chiral selectors to give protonated dimers were studied. The dissociation efficiency r (the intensity ratio of protonated dimers to protonated trimers) could be related to the enantiomeric excess (ee). The two enantiomerically pure L, D isomers and the racemic mixture are used as standards and the ee of the unknown sample is calculated using Eq. (21):

$$ee = 100 \left\{ \frac{1/(r_L - r_0) - 1/(r_D - r_0)}{2/(r - r_0) - 1/(r_L - r_0) - 1/(r_D - r_0)} \right\} \tag{21}$$

Using these methods, the authors have shown that the ee of an unknown mixture can be determined within 2% error.

Gas-phase chiral differentiation of amino acid guests in cyclodextrin hosts was reported by Lebrilla and coworkers [174,175]. Enantioselectivity is defined as the ratio of the rate constants (k_L/k_D) in gas-phase guest exchange reactions. The enantioselectivity was found to correlate with the number of carbon atoms in the side chain of amino acid, with the size of the amino acid and with the cavity size of the host. Ramirez et al. [174] isolated amino acid–cyclodextrin complexes in an FT-ICR cell and followed exchange reactions with amines (Eq. (22)) as a function of time. Rate constants were obtained from the slope of a plot of $\ln(I/I_0)$ vs. t, where I is the intensity of the complex at time t and I_0 is the sum of the intensities of the product and the starting complex

$$[\mathrm{CD : AA + H}]^+ + \mathrm{B} \overset{(a)}{\rightleftharpoons} [\mathrm{CD : AAH \cdots B}]^+ \overset{(b)}{\rightleftharpoons} [\mathrm{CD : BH \cdots AA}]^+ \overset{(c)}{\rightleftharpoons} [\mathrm{CD : B + H}]^+ + \mathrm{AA} \quad (22)$$

Exchange reaction rates were found to differ depending on the chirality of the amino acid guests. The L isomer showed enhanced reactivity compared to the D isomer in the cases of Ala and Val.

The same group studied the mechanism of chiral recognition in the gas phase using FT-ICR mass spectrometry [175]. Chiral discrimination requires that the host and the guest form reasonably stable complexes which involves the co-operative interaction of several weak forces such as dipole–dipole, hydrophobic, electrostatic, van der Waals and hydrogen bonding. A three point interaction model is generally used to describe these interactions in solution-state studies. Fig. 11 shows the lowest energy structure for enantiomeric pairs of Phe with β-cyclodextrin.

The Lebrilla group also reported a mass spectrometric method based on the guest exchange reaction for determining enantiomeric excess in mixtures of amino acids [176]. A calibration curve employing varying mixtures of D- and L-isomers was produced by plotting $I_R/(I_R + I_P)$ vs. the mole fraction of D, where I_R is the intensity of the reactant complex and I_P is the intensity of the product. These calibration curves were used to determine the enantiomeric excess in unknown mixtures.

A single publication on differentiation of enantiomers using MALDI mass spectrometry has appeared in the literature [177]. Cyclodextrin was used as the complexing agent to differentiate pseudo-enantiomeric mixtures. The chiral selectivity of cyclodextrin towards an amino acid was quantitatively estimated from the relative peak intensities of the two diastereomeric complexes in the MALDI mass spectrum. They could be differentiated by their mass

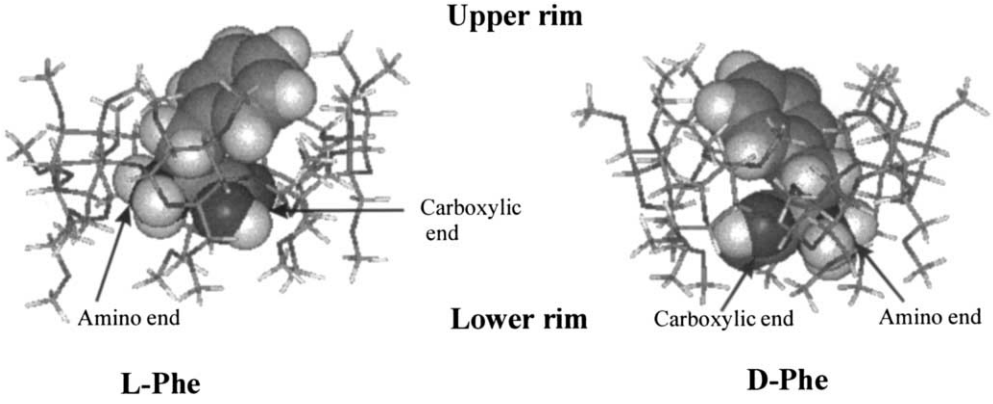

Fig. 11. Lowest energy structure for enantiomeric pairs of Phe with β-cyclodextrin ($[\mathrm{CD–Phe + H}]^+$). Reproduced with permission of Elsevier Science from [175]. Copyright 2001, by the American Society for Mass Spectrometry.

because one of the enantiomers was *n*-fold deuterated (D_n). The values of I_D/I_{L-D_n} or I_{D-D_n}/I_L show that cyclodextrins exhibit a preference towards L amino acids. The production of specific cyclodextrin inclusion complexes by MALDI–MS is still debated. For example, Lehmann et al. [49] found that tripeptide–β-cyclodextrin complexes that are known to exist in solution do not survive the MALDI sample preparation and ionization process. It is currently unclear under what conditions such a hydrophobic complex can be put into the gas phase by MALDI. It is possible that it is simply a matter of sample preparation: Lehmann et al. [49] used the dried droplet method, whereas So et al. [177] who clearly observed enantiomeric differentiation of amino acids in the presence of cyclodextrin used the layered sample preparation method.

5. Critical evaluation and summary

Soft ionization mass spectrometry is increasingly used to determine binding constants/binding energies of noncovalent complexes. As we have shown, one must distinguish between MS methods that measure the dissociation energies of gas-phase complex ions, and MS-based methods used for monitoring solution equilibria. For the latter, results generally agree well with known solution-phase thermodynamic values. On the other hand, gas-phase MS methods yield interaction energies that typically do not agree with solution-phase values. This is not surprising, because ionic or ion–dipole interactions will become stronger in the absence of screening by solvent, while other interactions such as hydrophobic interactions are destabilized in the absence of solvent. A direct comparison should therefore not be attempted, except in cases where one expects to learn something about the nature of the noncovalent interactions. The determination of gas-phase binding energies is expected to be very useful for rapid screening of therapeutic agents whose mode of interaction is designed to be mostly ionic or ion–dipole. In addition, experimental values for gas-phase binding energies can be directly compared to quantum mechanical computations that are typically obtained without incorporating solvent.

Frequently, qualitative trends in binding strength are reported rather than numbers for dissociation/association constants, binding enthalpies, or free energies. The reason, we believe is that this field is in the early stages of development, or in a kind of validation phase. One obvious problem is that ionization efficiencies/transfer coefficients are not generally taken into account. However, it has been shown for many systems that they significantly affect the determination of association constants by mass spectrometric methods. Another shortcoming is that a couple of representative peaks in the mass spectrum are often used to determine these trends, whereas taking all relevant peaks (higher order adducts, fragments, other charge states in ESI, etc.) belonging to a certain species would be accurate to quantitatively account for it. We are convinced that many of the existing published data could be evaluated (more) quantitatively.

By changing experimental parameters such as the cone voltage in an ESI experiment, a mass spectrometric analog to a melting curve can be constructed. From the slope of this melting curve at the point of 50% dissociation, it should be possible to derive a ΔH value in complete analogy to Eq. (1) [68]. For this purpose, a number of possibilities exist: thermal dissociation by HCD is one that has been already discussed. Furthermore, it is known that the plume temperature in MALDI is very close to the sublimation temperature of the matrix used [131]. Thus, different MALDI matrices could also lead to different degrees of complex dissociation by virtue of their sublimation temperature. The result will always be a kind of (gas-phase) melting curve.

Advice for planning future experiments and for appropriate data evaluation includes the following points: (i) assumptions for data evaluation must always be stated explicitly; this is often not the case in published studies. In order to obtain reliable results and for statistical reasons, measurements should be repeated several times; (ii) MALDI (and other methods, such as LILBID) should be developed more vigorously for studying noncovalent interactions of

biomacromolecules. MALDI is more tolerant to salts and buffers, often necessary ingredients for stabilizing complexes, and has thus some advantages over ESI in special situations; (iii) last but not least, we believe that the time is ripe for combining high accuracy methods such as the kinetic method or guided ion beam mass spectrometry with MALDI or ESI ion sources to study higher molecular weight complexes of biochemical interest.

Acknowledgements

We would like to thank Prof. M. Gross, Dr. T.J.D. Jørgensen, Prof. C. Lebrilla, Dr. V. Nesatyy, Prof. C. Robinson, Prof. K. Standing, and Prof. A. van Dorsellaer for providing figures for this review. Financial support for this work from the Swiss National Science foundation (Grant no. 2000-058861) is greatfully acknowledged.

References

[1] P. Hensley, Structure 4 (1996) 367.
[2] R.D. Smith, Z. Zhang, Mass Spectrom. Rev. 13 (1994) 411.
[3] D.L. Smith, Y. Deng, Z. Zhang, J. Mass Spectrom. 32 (1997) 135.
[4] Y. Liu, D.L. Smith, J. Am. Soc. Mass Spectrom. 5 (1994) 19.
[5] A.A. Rostom, P. Fucini, D.R. Benjamin, R. Juenemann, K.H. Nierhaus, F.U. Hartl, C.M. Dobson, C.V. Robinson, Proc. Natl. Acad. Sci. U.S.A. 97 (2000) 5185.
[6] M.A. Tito, K. Tars, K. Valegard, J. Hajdu, C.V. Robinson, J. Am. Chem. Soc. 122 (2000) 3550.
[7] W.J.H. Van Berkel, R.H.H. Van Den Heuvel, C. Versluis, A.J.R. Heck, Protein Sci. 9 (2000) 435.
[8] R.L. Winston, M.C. Fitzgerald, Mass Spectrom. Rev. 16 (1997) 165.
[9] F.W. McLafferty, Science 214 (1981) 280.
[10] J.A. Loo, Mass Spectrom. Rev. 16 (1997) 1.
[11] F.W. McLafferty, J. Am. Soc. Mass Spectrom. 8 (1997) 1.
[12] G. Siuzdak, Proc. Natl. Acad. Sci. U.S.A. 91 (1994) 11290.
[13] M. Karas, D. Bachmann, U. Bahr, F. Hillenkamp, Int. J. Mass Spectrom. Ion Proc. 78 (1987) 53.
[14] K. Tanaka, H. Waki, Y. Ido, S. Akita, Y. Yoshida, T. Yoshida, Rapid Commun. Mass Spectrom. 2 (1988) 151.
[15] F. Hillenkamp, M. Karas, R.C. Beavis, B.T. Chait, Anal. Chem. 63 (1991) 1193A.
[16] R. Zenobi, R. Knochenmuss, Mass Spectrom. Rev. 17 (1998) 337.
[17] J.B. Fenn, M. Mann, C.K. Meng, F.S. Wong, C.M. Whitehouse, Science 246 (1989) 64.
[18] J.B. Fenn, M. Mann, C.K. Meng, F.S. Wong, C.M. Whitehouse, Mass Spectrom. Rev. 9 (1990) 37.
[19] B. Ganem, Y.T. Li, J.D. Henion, J. Am. Chem. Soc. 113 (1991) 6294.
[20] W. Kleinekofort, J. Avdiev, B. Brutschy, Int. J. Mass Spectrom. Ion Proc. 152 (1996) 135.
[21] W. Kleinekofort, A. Pfenninger, T. Plomer, C. Griesinger, B. Brutschy, Int. J. Mass Spectrom. Ion Proc. 156 (1996) 195.
[22] F. Sobott, W. Kleinekofort, B. Brutschy, Anal. Chem. 69 (1997) 3587.
[23] A. Wattenberg, F. Sobott, H.D. Barth, B. Brutschy, Int. J. Mass Spectrom. 203 (2000) 49.
[24] R.A.W. Johnstone, I.A.S. Lewis, Int. J. Mass Spectrom. Ion Phys. 46 (1983) 451.
[25] R.A.W. Johnstone, I.A.S. Lewis, M.E. Rose, Tetrahedron 39 (1983) 1597.
[26] G. Bonas, C. Bosso, M.R. Vignon, J. Incl. Phen. Mol. Recog. Chem. 7 (1989) 637.
[27] V.F. Man, J.D. Lin, K.D. Cook, J. Am. Chem. Soc. 107 (1985) 4635.
[28] M. Przybylski, M.O. Glocker, Angew. Chem., Int. Ed. 35 (1996) 806.
[29] R.D. Smith, J.E. Bruce, Q. Wu, Q.P. Lei, Chem. Soc. Rev. 26 (1997) 191.
[30] B.N. Pramanik, P.L. Bartner, U.A. Mirza, Y.-H. Liu, A.K. Ganguly, J. Mass Spectrom. 33 (1998) 911.
[31] F. Hillenkamp, in: W. Ens, K.G. Standing, I.V. Chernushevich (Eds.), New Methods for the Study of Biomolecular Complexes, Kluwer Academic Publishers, Dordrecht, The Netherlands, 1998.
[32] J.N. Israelachvili, Intermolecular and Surface Forces, Academic Press, London, 1991.
[33] M.T. Rodgers, P.B. Armentrout, Mass Spectrom. Rev. 19 (2000) 215.
[34] J.B. Cunniff, P. Vouros, J. Am. Soc. Mass Spectrom. 6 (1995) 437.
[35] W.D. Lehmann, Massenspektrometrie in der Biochemie, Spektrum Analytik, Akad. Verl., Heidelberg, 1996.
[36] J.R. Kimmel, Meth. Enzymol. 11 (1967) 584.
[37] H.A. Itano, R.A. Robinson, J. Biol. Chem. 247 (1972) 4819.
[38] M. Kalkum, M. Przybylski, M.O. Glocker, Bioconjugate Chem. 9 (1998) 226.
[39] M. Galvani, M. Hamdan, P.G. Righetti, Rapid Commun. Mass Spectrom. 14 (2000) 1925.
[40] H. Belva, C. Valois, C. Lange, Rapid Commun. Mass Spectrom. 14 (2000) 224.
[41] M. Münchbach, M. Quadroni, G. Miotto, P. James, Anal. Chem. 72 (2000) 4047.
[42] S.D. Friess, R. Zenobi, J. Am. Soc. Mass Spectrom. 12 (2001) 810.
[43] S.D. Friess, J.M. Daniel, R. Hartmann, R. Zenobi, Int. J. Mass Spectrom., in press.
[44] A.A. Rostom, J.R.H. Tame, J.E. Ladbury, C.V. Robinson, J. Mol. Biol. 296 (2000) 269.

[45] K.O. Börnsen, in: J.R. Chapman (Ed.), Methods in Molecular Biology, Vol. 146, Humana Press, Totowa, NJ, 2000.
[46] B. Salih, R. Zenobi, Anal. Chem. 70 (1998) 1536.
[47] R.D. Smith, K.J. Light-Wahl, Biol. Mass Spectrom. 22 (1993) 493.
[48] E. Lehmann, R. Zenobi, S. Vetter, J. Am. Soc. Mass Spectrom. 10 (1999) 27.
[49] E. Lehmann, B. Salih, M. Gomez-Lopez, F. Diederich, R. Zenobi, Analyst 125 (2000) 849.
[50] T. Vogt, J. Roth, C. Sorg, F. Hillenkamp, K. Strupat, J. Am. Soc. Mass Spectrom. 10 (1999) 1124.
[51] K. Strupat, H. Rogniaux, A. Van Dorsselaer, J. Roth, T. Vogl, J. Am. Soc. Mass Spectrom. 11 (2000) 780.
[52] J. Gross, A. Leisner, F. Hillenkamp, S. Hahner, M. Karas, J. Schäfer, F. Lützenkirchen, E. Nordhoff, J. Am. Soc. Mass Spectrom. 9 (1998) 866.
[53] N. Potier, P. Barth, D. Tritsch, J.F. Biellmann, A. Van Dorsselaer, Eur. J. Biochem. 243 (1997) 274.
[54] M. Przybylski, V. Schnaible, J. Kast, S. Bohler, J. Michels, A. Wattenberg, T.A. Fligge, D. Forst, K. Diederichs, U. Nestel, K. Zeth, M.O. Glocker, W. Welte, NATO ASI Ser. C 510 (1998) 17.
[55] M. Przybylski, Adv. Mass Spectrom. 13 (1995) 257.
[56] A.G. Marshall, M.R. Emmett, M.A. Freitas, C.L. Hendrickson, Z. Zhang, in: A.L. Burlingame, S.A. Carr, M.A. Baldwin (Eds.), Mass Spectrometry in Biology and Medicine, Humana Press, Totowa, NJ, 2000.
[57] S. Akashi, K. Takio, Protein Sci. 9 (2000) 2497.
[58] A. Li, C. Fenselau, I.A. Kaltashov, Proteins: Struct., Funct., Genet. (Suppl. 2) (1998) 22.
[59] I.A. Kaltashov, C. Fenselau, Proteins: Struct., Funct., Genet. 27 (1998) 165.
[60] R.B. Cole, Electrospray Ionization Mass Spectrometry: Fundamentals, Instrumentation and Applications, Wiley, New York, 1997.
[61] J.S. Brodbelt, Int. J. Mass Spectrom. 200 (2000) 57.
[62] R. Guevremont, K.W.M. Siu, J.C.Y. Le Blanc, S.S. Berman, J. Am. Soc. Mass Spectrom. 3 (1992) 216.
[63] E. Leize, A. Jaffrezic, A. Van Dorsselaer, J. Mass Spectrom. 31 (1996) 537.
[64] K.A. Sannes-Lowery, P. Hu, D.P. Mack, H.-Y. Mei, J.A. Loo, Anal. Chem. 69 (1997) 5130.
[65] C.V. Robinson, E.W. Chung, B.B. Kragelund, J. Knudsen, R.T. Aplin, F.M. Poulsen, C.M. Dobson, J. Am. Chem. Soc. 118 (1996) 8646.
[66] Y.-T. Li, Y.-L. Hsieh, J.D. Henion, T.D. Ocain, G.A. Schiehser, B. Ganem, J. Am. Chem. Soc. 116 (1994) 7487.
[67] H. Wang, G.R. Agnes, Anal. Chem. 71 (1999) 3785.
[68] L.A. Marky, K.J. Breslauer, Biopolymers 26 (1987) 1601.
[69] X. Cheng, Q. Gao, R.D. Smith, K.-E. Jung, C. Switzer, Chem. Commun. (1996) 747.
[70] M. Fändrich, M.A. Tito, M.R. Leroux, A.A. Rostom, F.U. Hartl, C.M. Dobson, C.V. Robinson, Proc. Natl. Acad. Sci. U.S.A. 97 (2000) 14151.
[71] H.-K. Lim, Y.L. Hsieh, B. Ganem, J. Henion, J. Mass Spectrom. 30 (1995) 708.
[72] M.J. Greig, H.-J. Gaus, L.L. Cummins, H. Sasmor, R.H. Griffey, J. Am. Chem. Soc. 117 (1995) 10765.
[73] K.A. Sannes-Lowery, R.H. Griffey, S.A. Hofstadler, Anal. Biochem. 280 (2000) 264.
[74] K. Eckart, J. Spiess, J. Am. Soc. Mass Spectrom. 6 (1995) 912.
[75] J.A. Loo, P. Hu, P. McConnell, W.T. Mueller, J. Am. Soc. Mass Spectrom. 8 (1997) 234.
[76] A. Ayed, A.N. Krutchinsky, W. Ens, K.G. Standing, H.W. Duckworth, Rapid Commun. Mass Spectrom. 12 (1998) 339.
[77] R.H. Griffey, S.A. Hofstadler, K.A. Sannes-Lowery, D.J. Ecker, S.T. Crooke, Proc. Natl. Acad. Sci. U.S.A. 96 (1999) 10129.
[78] N. Carte, F. Legendre, E. Leize, N. Potier, F. Reeder, J.-C. Chottard, A. Van Dorsselaer, Anal. Biochem. 284 (2000) 77.
[79] D.-S. Young, H.-Y. Hung, L.K. Liu, J. Mass Spectrom. 32 (1997) 432.
[80] F. Dubois, R. Knochenmuss, R. Zenobi, Eur. Mass Spectrom. 5 (1999) 267.
[81] T.J.D. Jørgensen, P. Roepstorff, A.J.R. Heck, Anal. Chem. 70 (1998) 4427.
[82] T.J.D. Jørgensen, T. Staroske, P. Roepstorff, D.H. Williams, A.J.R. Heck, J. Chem. Soc., Perkin Trans. 2 (1999) 1859.
[83] E.C. Kempen, J.S. Brodbelt, Anal. Chem. 72 (2000) 5411.
[84] G.W. Gokel, D.M. Goli, C. Mingati, L. Echegoyen, J. Am. Chem. Soc. 105 (1983) 6786.
[85] C.M. Goff, M.A. Matchetter, N. Shabestary, S. Khazaeli, Polyhedron 15 (1996) 3897.
[86] D. Giraud, O. Laprévote, B.C. Das, Org. Mass Spectrom. 29 (1994) 169.
[87] M.L. Reyzer, J.S. Brodbelt, A.P. Marchand, Z. Chen, Z. Huang, I.N.N. Namboothiri, Int. J. Mass. Spectrom. 204 (2001) 133.
[88] D.-S. Young, H.-Y. Hung, L.K. Liu, Rapid Commun. Mass Spectrom. 11 (1997) 769.
[89] S.M. Blair, E.C. Kempen, J.S. Brodbelt, J. Am. Soc. Mass Spectrom. 9 (1998) 1049.
[90] K. Wang, G.W. Gokel, J. Org. Chem. 61 (1996) 4693.
[91] S.F. Ralph, P. Iannitti, R. Kanitz, M.M. Sheil, Eur. Mass Spectrom. 2 (1996) 173.
[92] E.C. Kempen, J.S. Brodbelt, R.A. Bartsch, M.T. Blanda, D.B. Farmer, Anal. Chem. 73 (2001) 384.
[93] S.M. Blair, J.S. Brodbelt, A.P. Marchand, H.-S. Chong, S. Alihodzic, J. Am. Soc. Mass Spectrom. 11 (2000) 884.
[94] E. Kempen, J.S. Brodbelt, R.A. Bartsch, Y. Jang, J.S. Kim, Anal. Chem. 71 (1999) 5493.
[95] S.M. Blair, J.S. Brodbelt, A.P. Marchand, K.A. Kumar, H.-S. Chong, Anal. Chem. 72 (2000) 2433.
[96] A. Reichert, R. Fröhlich, R. Ferguson, A. Kraft, J. Chem. Soc., Perkin Trans. 1 (2001) 1321.
[97] L. Peters, R. Froehlich, A.S.F. Boyd, A. Kraft, J. Org. Chem. 66 (2001) 3291.
[98] M.T. Blanda, D.B. Farmer, J.S. Brodbelt, B.J. Goolsby, J. Am. Chem. Soc. 122 (2000) 1486.

[99] S.M. Blair, J.S. Brodbelt, G.M. Reddy, A.P. Marchand, J. Mass Spectrom. 33 (1998) 721.
[100] J.S. Brodbelt, E. Kempen, M. Reyzer, Struct. Chem. 10 (1999) 213.
[101] C.A. Schalley, T. Martín, U. Obst, J. Rebek Jr., J. Am. Chem. Soc. 121 (1999) 2133.
[102] A. Triolo, F.M. Arcamone, A. Raffaelli, P. Alvadori, J. Mass Spectrom. 32 (1997) 1186.
[103] K.A. Sannes-Lowery, H.-Y. Mei, J.A. Loo, Int. J. Mass Spectrom. 193 (1999) 115.
[104] V. Gabelica, E. De Pauw, F. Rosu, J. Mass Spectrom. 34 (1999) 1328.
[105] O. Baudoin, F. Gonnet, M.-P. Teulade-Fichou, J.-P. Vigneron, J.-C. Tabet, J.-M. Lehn, Chem. Eur. J. 5 (1999) 2762.
[106] A. Kapur, J.L. Beck, M.M. Sheil, Rapid Commun. Mass Spectrom. 13 (1999) 2489.
[107] K.X. Wan, T. Shibue, M.L. Gross, J. Am. Chem. Soc. 122 (2000) 300.
[108] Y.L. Hsieh, Y.T. Li, J.D. Henion, B. Ganem, Biol. Mass Spectrom. 23 (1994) 272.
[109] J. Gao, X. Cheng, G.B. Sigal, J.E. Bruce, B.L. Schwartz, S.A. Hofstadler, G.A. Anderson, R.D. Smith, G.M. Whitesides, J. Med. Chem. 39 (1996) 1949.
[110] X. Cheng, R. Chen, J.E. Bruce, B.L. Schwartz, G.A. Anderson, S.A. Hofstadler, D.C. Gale, R.D. Smith, J. Am. Chem. Soc. 117 (1995) 8859.
[111] B.J. Goolsby, J.S. Brodbelt, E. Adou, M. Blanda, Int. J. Mass Spectrom. 193 (1999) 197.
[112] Q. Wu, J. Gao, D. Joseph-McCarthy, G.B. Sigal, J.E. Bruce, G.M. Whitesides, R.D. Smith, J. Am. Chem. Soc. 119 (1997) 1157.
[113] H. Rogniaux, A. Van Dorsselaer, P. Barth, J.F. Biellmann, J. Barbanton, M. van Zandt, B. Chevrier, E. Howard, A. Mitschler, N. Potier, L. Urzhumtseva, D. Moras, A. Podjarny, J. Am. Soc. Mass Spectrom. 10 (1999) 635.
[114] C.L. Hunter, A.G. Mauk, D.J. Douglas, Biochemistry 36 (1997) 1018.
[115] V. Gabelica, E. De Pauw, J. Mass Spectrom. 36 (2001) 397.
[116] A.K. Shukla, J.H. Futrell, J. Mass Spectrom. 35 (2000) 1069.
[117] Y.-L. Chen, J.M. Campbell, B.A. Collings, L. Konermann, D.J. Douglas, Rapid Commun. Mass Spectrom. 12 (1998) 1003.
[118] S.G. Penn, F. He, M.K. Green, C.B. Lebrilla, J. Am. Soc. Mass Spectrom. 8 (1997) 244.
[119] I. Apostol, Anal. Biochem. 272 (1999) 8.
[120] T.J.D. Jørgensen, D. Delforge, J. Remacle, G. Bojesen, P. Roepstorff, Int. J. Mass Spectrom. 188 (1999) 63.
[121] A. van der Kerk-van Hoof, A.J.R. Heck, J. Mass Spectrom. 34 (1999) 813.
[122] K.X. Wan, M.L. Gross, T. Shibue, J. Am. Soc. Mass Spectrom. 11 (2000) 450.
[123] J. Gao, Q. Wu, J. Carbeck, Q.P. Lei, R.D. Smith, G.M. Whitesides, Biophys. J. 76 (1999) 3253.
[124] V.J. Nesatyy, J. Mass Spectrom. 36 (2001) 950.
[125] K.M. Ervin, P.B. Armentrout, J. Chem. Phys. 83 (1985) 166.
[126] R.H. Schultz, K.C. Crellin, P.B. Armentrout, J. Am. Chem. Soc. 113 (1991) 8590.
[127] P.B. Armentrout, in: N.G. Adams, L.M. Babock (Eds.), Advances in Gas Phase Ion Chemistry, Vol. 1, JAI, Greennwich, 1992.
[128] M.T. Rodgers, K.M. Ervin, P.B. Armentrout, J. Chem. Phys. 106 (1997) 4499.
[129] K. Ervin, Chem. Rev. 101 (2001) 391.
[130] M.T. Rodgers, P.B. Armentrout, J. Am. Chem. Soc. 122 (2000) 8548.
[131] C.D. Mowry, M.V. Johnston, J. Phys. Chem. 98 (1994) 1904.
[132] V. Frankevich, R. Zenobi, Rapid Commun. Mass Spectrom. 15 (2001) 2035.
[133] R.C. Dunbar, T.B. McMahon, Science 279 (1998) 194.
[134] S.E. Rodriguez-Cruz, J.S. Klassen, E.R. Williams, J. Am. Soc. Mass Spectrom. 8 (1997) 565.
[135] Y. Ge, D.M. Horn, F.W. McLafferty, Int. J. Mass Spectrom. 210/211 (2001) 203.
[136] D.S. Gross, Y. Zhao, E.E. Williams, J. Am. Soc. Mass Spectrom. 8 (1997) 519.
[137] P.D. Schnier, J.S. Klassen, E.F. Strittmatter, E.R. Williams, J. Am. Chem. Soc. 120 (1998) 9605.
[138] J.S. Klassen, P.D. Schnier, E.R. Williams, J. Am. Soc. Mass Spectrom. 9 (1998) 1117.
[139] E.F. Strittmatter, P.D. Schnier, J.S. Klassen, E.R. Williams, J. Am. Soc. Mass Spectrom. 10 (1999) 1095.
[140] W.D. Price, R.A. Jockusch, E.R. Williams, J. Am. Chem. Soc. 120 (1998) 3474.
[141] N. Felitsyn, E.N. Kitova, J.S. Klassen, Anal. Chem. 73 (2001) 4647.
[142] E.N. Kitova, P.I. Kitov, D.R. Bundle, J.S. Klassen, Glycobiology 11 (2001) 605.
[143] F. He, J. Ramirez, B.A. Garcia, C.B. Lebrilla, Int. J. Mass Spectrom. 182 (1999) 261.
[144] B. Garcia, J. Ramirey, S. Wong, C.B. Lebrilla, Int. J. Mass Spectrom. 210/211 (2001) 215.
[145] R.L. Woodin, J.L. Beauchamp, J. Am. Chem. Soc. 100 (1978) 501.
[146] A.W.P.M. Holland, D.M. Lindsay, K.I. Peterson, A.W. Castleman Jr., J. Am. Chem. Soc. 109 (1978) 6039.
[147] L. Sallans, K.R. Lane, B.S. Freiser, J. Am. Chem. Soc. 111 (1989) 865.
[148] W.J. van der Hart, Mass Spectrom. Rev. 8 (1989) 237.
[149] K.F. Willey, P.Y. Cheng, M.B. Bishop, M.A. Duncan, J. Am. Chem. Soc. 113 (1991) 4721.
[150] J.D. Faulk, R.C. Dunbar, J. Am. Chem. Soc. 114 (1992) 8596.
[151] S. Afzaal, B.S. Freiser, Chem. Phys. Lett. 218 (1994) 254.
[152] R.G. Cooks, J.S. Patrick, T. Kotiaho, S.A. McLuckey, Mass Spectrom. Rev. 13 (1994) 287.
[153] R.G. Cooks, P.S.H. Wong, Acc. Chem. Res. 31 (1998) 379.
[154] R.G. Cooks, J.T. Koskinen, P.D. Thomas, J. Mass Spectrom. 34 (1999) 85.
[155] W.R. Davidson, P. Kebarle, J. Am. Chem. Soc. 98 (1976) 6133.

[156] I. Dzidic, P. Kebarle, J. Phys. Chem. 74 (1970) 1466.
[157] F. Bouchard, J.W. Hepburn, T.B. McMahon, J. Am. Chem. Soc. 111 (1989) 8934.
[158] P.R. Kemper, J. Bushnell, P. Van Koppen, M.T. Bowers, J. Phys. Chem. 97 (1993) 1810.
[159] J.E. Bushnell, P.R. Kemper, M.T. Bowers, J. Phys. Chem. 99 (1995) 15602.
[160] M. Peschke, A.T. Blades, P. Kebarle, J. Phys. Chem. A 102 (1998) 9978.
[161] S. Hoyau, K. Norrman, T.B. McMahon, G. Ohanessian, J. Am. Chem. Soc. 121 (1999) 8864.
[162] B.A. Cerda, C. Wesdemiotis, J. Am. Chem. Soc. 117 (1995) 9734.
[163] O.V. Nemirovskiy, R. Ramanathan, M.L. Gross, J. Am. Soc. Mass Spectrom. 8 (1997) 809.
[164] B.A. Cerda, S. Hoyau, G. Ohanessian, C. Wesdemiotis, J. Am. Chem. Soc. 120 (1998) 2437.
[165] B.A. Cerda, C. Wesdemiotis, J. Am. Chem. Soc. 118 (1996) 11884.
[166] J. Zhang, R. Knochenmuss, E. Stevenson, R. Zenobi, Int. J. Mass Spectrom. 213 (2002) 237.
[167] Y.-P. Ho, Y.-C. Yang, S.J. Klipperstein, R.C. Dunbar, J. Phys. Chem. A 101 (1997) 3338.
[168] B.P. Pozniak, R.C. Dunbar, J. Am. Chem. Soc. 119 (1997) 10439.
[169] V. Ryzhov, R.C. Dunbar, J. Am. Chem. Soc. 121 (1999) 2259.
[170] A. Filippi, A. Giardini, S. Piccirillo, M. Speranza, Int. J. Mass Spectrom. 198 (2000) 137.
[171] M. Sawada, Mass Spectrom. Rev. 16 (1997) 73.
[172] Z.P. Yao, T.S. Wan, K.P. Kwong, C.T. Che, Anal. Chem. 72 (2000) 5383.
[173] Z.P. Yao, T.S. Wan, K.P. Kwong, C.T. Che, Anal. Chem. 72 (2000) 5394.
[174] J. Ramirez, F. He, C.B. Lebrilla, J. Am. Chem. Soc. 120 (1998) 7387.
[175] S. Ahn, J. Ramirez, G. Grigorean, C.B. Lebrilla, J. Am. Soc. Mass Spectrom. 12 (2001) 278.
[176] G. Grigorean, J. Ramirez, S. Ahn, C.B. Lebrilla, Anal. Chem. 72 (2000) 4275.
[177] M.P. So, T.S.M. Wan, T.-W.D. Chan, Rapid Commun. Mass Spectrom. 14 (2000) 692.